Till as — AD-736604
NASA CR-120844

NOLTR 71-228

THE NOL BALLISTIC PISTON COMPRESSOR II. OPERATION UP TO 5,000 ATM

By
Gordon L. Hammond
George T. Lalos

16 DECEMBER 1971

NOL

NAVAL ORDNANCE LABORATORY, WHITE OAK, SILVER SPRING, MARYLAND

APPROVED FOR PUBLIC RELEASE;
DISTRIBUTION UNLIMITED

NOLTR 71-228

THE NOL BALLISTIC PISTON COMPRESSOR II. OPERATION UP TO 5,000 ATM.

by:
Gordon L. Hammond
and
George T. Lalos

ABSTRACT: Experiments are described which demonstrated the feasibility of rapidly compressing inert gases in a ballistic piston compressor to simultaneously high temperatures and densities previously unobtainable in the laboratory. With argon, temperatures of the order of 6000°K and accompanying densities of the order of 100 Amagats have been obtained; and with nitrogen, temperatures and densities of 3000°K and 400 Amagats have been approached. Details of the design, assembly, instrumentation, and operating procedures are presented, and the results of mechanical and thermal performance tests up to 5000 atmospheres pressure are described. Emphasis is placed on experiments which demonstrated the usefulness of this apparatus for spectral line broadening studies.

Interagency Number C-7757B
Technical Management
NASA Lewis Research Center
R. W. Patch

APPROVED BY: CARL BOYARS, Chief
Advanced Chemistry Division
Chemistry Research Department
Naval Ordnance Laboratory
Silver Spring, Maryland 20910

NOLTR 71-228 16 December 1971

THE NOL BALLISTIC PISTON COMPRESSOR II. OPERATION UP TO 5000 ATM.

The work described in this report was carried out primarily under Task IR 167, Spectroscopic Studies of High Pressure Gases. The techniques described here produce hot, dense gases that simulate the conditions found in explosive detonations, nuclear rocket engines, and imploding underwater bubbles. Portions of this work were funded by the National Aeronautics and Space Administration.

ROBERT WILLIAMSON II
Captain, USN
Commander

Albert Lightbody

ALBERT LIGHTBODY
By direction

TABLE OF CONTENTS

TABLE OF CONTENTS (Cont'd)

FIGURES

I. INTRODUCTION

The task of the Spectroscopy Group of the Advanced Chemistry Division is to investigate the nature of the radiation emitted by hot, compressed gases. The investigation involves detailed observations and interpretations of the shapes, widths and shifts of the spectral lines emitted by these gases. The hot, dense gas is obtained by a rapid, quasi-adiabatic compression in a ballistic piston compressor, a detailed description of the design, construction and operation of which is the subject of this report.

In the course of the investigation, it became apparent that the original compressor,[1] which had been designed and used for equation of state measurements on compressed gases,[2] was inadequate for radiation studies. Specifically, its stroke was so short that at pressures of greater than 1000 atm the radiating gases emitted inadequate light fluxes for photographic work. Furthermore, the reservoir which contained the piston driving gas had a low pressure limit, which in turn limited maximum pressures obtainable, and it was inconvenient to make changes in pistons, windows, and transducers without wasting large quantities of gas. Therefore, it was necessary to design and build a more versatile compressor capable of producing wider ranges of temperature and pressure, and incorporating improvements in the optical and operational features. The original design requirements and specifications are discussed more fully in reference 3.

II. ASSEMBLY AND OPERATING PROCEDURES

Initial Assembly

The compressor that was designed and constructed is shown assembled in Fig. 1, details of the reservoir and piston release section are shown in Fig. 2, and Fig. 3 shows details of the initial high pressure section assembly. After the delivery and a detailed inspection of all the parts had been completed, assembly and alignment of the various components began. Starting with the rear table and reservoir carriage, precision bubble levels were used to position the axes and surfaces, with respect to the horizontal plane, of the reservoir and piston release section, the tube, high pressure section, and finally the front carriage and table. Steel shims were necessary to align the reservoir and the high pressure section with their respective carriages. The brass plug described in reference 3 for testing the straightness of the tube bore was also used to test the alignment of the high pressure section with respect to the tube.

The final tests prior to actual operation were static pressure tests for leaks. All assemblies were statically pressurized to approximately 70 atmospheres with He, and the only detectable leak was at the sealing surface of the Kistler quartz crystal pressure transducer installed in the end-plug. This leak was eliminated by removing a burr found on the mating surface of the transducer adapter. It was also found that the tube and high pressure section could be evacuated to a pressure of less than 1 mm Hg, and which could be maintained for periods of a few minutes after stopping the vacuum pump.

Basic Operating Procedures

The general principles involved in the operation of this apparatus are described in reference 3. To supplement that report, a detailed operating procedure has been prepared and is prominently displayed on the compressor control panel along with a gas line schematic diagram, Fig. 4, showing all gas line connections, pressure gages, and valves. This standard operating procedure (SOP) emphasizes the safety precautions to be taken, and it is revised whenever a

significantly different procedure is introduced. The SOP describes the preparation of the compressor prior to a shot, the variations in the procedure required for unusual initial conditions of the test gas, and the procedure for disassembly in case cleaning or other maintenance is required. The SOP also contains a check-list of valve adjustments, electrical connections, photographic precautions, dial settings and safety checks, all of which must be attended to before firing.

The SOP describes the disassembly procedure up to the point where the piston may be removed from the tube. For cleaning the tube, the end plug closing the tube at the high pressure end must be removed by loosening the five set screws which prestress the Bridgman seal. The end cap holding the pressure transducer may then be screwed off. For a thorough cleaning the high pressure section must also be disconnected from the tube by unscrewing the front coupling nut. To perform maintenance on the piston release section, the reservoir gas must be exhausted to atmospheric pressure, and the pressure behind the plunger must also be released. The quick-opening solenoid valve whose opening initiates the firing of the piston down the tube, must then be removed, after which the entire piston release section and the front flange of the reservoir can be removed from the reservoir by removing the ten 1-1/8" nuts. The piston release section and flange assembly must be supported during this operation by suspending it from the hook of the 1/2-ton hoist which is attached to overhead tracks. When reassembling the piston release section and flange to the reservoir, proper alignment with the tube is obtained by allowing the assembly to rest on the bottom of the opening in the reservoir while tightening the 1-1/8" nuts.

Pistons

Although pistons used in this compressor have evolved from simple right circular cylinders to multi-component assemblies, they are nearly all based on the same set of design principles. With the exception of only the initial configuration, they all have short bearing surfaces composed of an alloy that slides well on steel

(aluminum or phosphor-bronze), with a small circumferential groove that induces turbulence in the leaking gas and catches small particles that might otherwise cause galling. The radial clearance between bearing surface and tube bore is 45 microns, although one successful test was made with a light piston having half that clearance. The main piston body and any material fastened to the piston face is undercut 150 microns from the tube bore. Strain gage measurements have shown that the test section expands slightly with the internal test gas pressure so that the piston/bore clearance is maintained in spite of axial compression and radial expansion of the piston at the moment of maximum gas compression.

The performance of individual piston types are discussed in other parts of this report. The simple cylindrical piston is mentioned in the Cleaning Procedures section of this chapter and was used in all the initial ballistic action tests described in chapter IV. Light pistons of various materials with undercut bodies are also described in chapter IV. Refractory piston head materials are discussed in chapter V, and flexible piston seals are discussed in chapter VI.

Cleaning Procedures

A small amount of fine metallic dust particles is formed during each shot by the rubbing of the piston bearing surfaces against the bore of the tube. If left to accumulate, these particles will partially vaporize during subsequent shots and contaminate the test gas ahead of the piston. These particles are effectively removed by pulling through the tube a tight-fitting swab of felt wrapped with wiping tissue and soaked with acetone or methanol. The last pass with the swab is usually made with ethanol.

There have been shots where the temperature of the test gas has been high enough to melt slightly the leading edge of the copper and copper-alloy pistons. During such shots a ring of copper is deposited in the bore of the high pressure section at the point where the leading edge of the piston comes to rest momentarily, the point at which maximum pressure, maximum temperature, maximum gas leakage rate across the piston, and, therefore, maximum heat transfer and

ablation take place. This deposit onto the chromium plated bore of the high pressure section is effectively removed by soaking the bore overnight in a warm bath of chromic acid.

In the early tests of compressor operation, pure copper pistons of right circular cylindrical geometry were used. These pistons deposited streaks and patches of copper metal along the tube bore, some of several feet in length. These deposits had to be removed by a honing operation, using a portable device[5] driven by a compressed air motor. However, if honing is required in the future, the NOL Technical Shops are now equipped to perform this operation.

Additives introduced into the test gas for spectroscopic studies are occasionally in the form of powdered crystalline solids or small metallic particles. They are usually removed as above, with the swab soaked with the appropriate solvent, such as acetone, methanol, ethanol, or distilled water. If the additives are some form of the alkali metals, the above procedures are not sufficient to remove all traces of the alkali, but the residual contamination is usually tolerable.

Introduction of Additives

In earlier versions of this compressor, additives were usually in the form of metal halide crystalline powders. The search for satellite bands of the alkali metals[6] and alkaline earth metals[7] was conducted this way by placing a few milligrams of the powdered salt near the end wall in the test section bore. Collision effects in the spectra of mercury[8], lead and cesium have also been observed by adding small quantities of the pure metal into the test section. The metal spectra that have been studied with the present compressor (NaI, CaI, CaII) have originated from ever present contaminants unavoidably introduced in cleaning procedures. From opacity measurements, the abundance of these contaminant vapors relative to that of the rare gas is approximately -9 dex(1 dex = one power of 10).

Additives used in recent experiments with the current compressor version have been in gaseous form. Mixtures of 10% and 20% H_2 in He were prepared by evacuating the tube and test section and filling

them to atmospheric pressure with H_2, then pumping down to 76 (or 152) mm Hg for 10% (or 20%) H_2, and then quickly filling back to 760 mm Hg with helium.[9] That procedure did not yield reproducible maximum pressures, and considerable improvement was obtained by filling the evacuated tube, test section and piston release section with premixed 10% and 20% H_2 in helium.[10]

A further gaseous additive procedure was developed for spectroscopic temperature measurements. In this work,[11] trace quantities of hydrocarbon vapors were mixed with the test gas, and upon compression and heating decomposition of C_2H_2 or of CH_4 yielded strong emission in the Swan band system of C_2. It was noted during this work that concentrations of either acetylene or methane greater than 400 ppm in helium yielded a layer of soot deposited on the walls of the test section. Mixtures of methane in helium in the concentration range from 225 to 40 ppm were prepared in a large steel mixing tank by adding premixed CH_4/He from commercially supplied calibrated mixtures and then diluting with pure helium to the desired concentration. The CH_4/He ratio was monitored just before introduction into the compressor with an emission spectroscopic scheme calibrated with the commercially supplied mixtures.[12]

8 Meter Tube

A study of the ultraviolet opacity of H_2 in support of NASA's gaseous core nuclear rocket program necessitated increasing the tube length from 4 meters to 8 meters.[10] This requirement results from the high volumetric compression ratios associated with low specific heat ratio gases, together with the 1 cm minimum piston/end-plug separation needed for test beam attenuation measurements.

An 8 meter tube (5 cm bore) consisting of two 4 meter tubes joined by a coupling nut was designed at NOL and fabricated by a commercial supplier.[13] Manufacturing tolerences were kept close in order to prevent the piston from becoming jammed during its high speed flight across the juncture point. A table is located under the coupling

nut and supports the center of the tube with a cradle/ball bushing arrangement similar to that employed to support the high pressure section and the reservoir. The new tube was installed, aligned and fired many times without any difficulties.

III. INSTRUMENTATION

The compressor has been instrumented with a variety of pressure gages, electrical transducers, and optical accessories. Although most of the instruments described here were purchased from commercial sources, no endorsement or recommendation is implied in their description. All instruments described here adequately performed their intended function, but in no instance was any evaluation or comparative test made on competitive products.

Mechanical and Electrical Devices

To measure the initial pressure of the test gas, an accurate aneroid manometer[14] is used. This gage has a range of 0-800 mm Hg pressure with 1 mm dial graduations and an accuracy of 0.1% of full scale. The gage used to measure reservoir gas pressure prior to firing is a precise bourdon tube gage.[15] This gage has a range of 0-150 standard atmospheres with 0.2 atm dial graduations and an accuracy of 0.1% of full scale.

Electrical transducers are used for dynamic pressure measurements during the compression cycles. Strain gage transducers[16] are occasionally installed in the piston release section to monitor the driving pressure and the pressure behind the plunger. Quartz crystal piezoelectric transducers[17] are mounted in the end wall of the high pressure section. The electrical analog signals from these transducers are displayed on oscilloscopes and photographed with Polaroid cameras. The quartz crystal gage signals are amplified, before display, by the electronic circuitry described in reference 18.

Other electrical transducers include a linear motion potentiometer[19] attached to the high pressure section. This device monitors the recoil motion of the compressor due to piston motion. Bonded strain gages[20] are occasionally cemented to the outside surface of the high pressure section to detect deformation due to internal pressure. These gages have also been employed at the piston release section to detect stresses transmitted from the high pressure region during compression cycles.

The position of the piston prior to firing is indicated by a light on the control panel which is controlled by a miniature switch in the piston release section. The electrical leads for the switch pass through a high pressure sealing gland[21] in the walls of the piston release section.

Optical Acessories

A variety of spectrographs are available to view the radiation emitted by the test gases. Two Bausch and Lomb instruments, a medium quartz prism and 1.5 meter concave grating, have relative aperture ratios of f/12 and f/24, respectively, while the Baird-Atomic 3-meter concave grating instrument has an aperture ratio of f/35. The principal spectrographic instrument available for spectral line shape studies is a McPherson Model 216 combination spectrograph-monochromator—polychromator with 1 meter focal length and aperture ratio of f/9. A wide variety of quartz and glass lenses are on hand for focussing the radiation onto the slits of these spectrographs, and occasionally front surface aluminized mirrors are used when the axes of the spectrographs cannot be parallel to the axis of the viewing window in the high pressure section. All external optical components are mounted on a frame that is isolated from the compressor and its supports and consequently they are free from vibrations associated with compressor operation.

The viewing windows are right circular cylinders, and are made of fused quartz or synthetic sapphire. Their thicknesses range from 10 to 19 mm and diameters from 19 to 31 mm. Both faces are optical flats, the edges are chamfered for stress relief, and the materials are as free of striations and bubbles as possible. In assembly, one face of the window bears against the optically flat surface of the steel window support and forms a reliable gas seal. An O-ring seal was later added to the window support to prevent leaks during evacuation of the high pressure section. The window support has a 1-cm diameter hole through which the radiation passes and is sealed by a conventional Bridgman seal.

A variety of light sources and calibration devices are on hand for producing wavelength and intensity calibration spectra. These include:

1. A high intensity, stable, d.c. carbon arc.[22]
2. An O_2/H_2 and O_2/C_2H_2 flame source with atomizer-burners for aspirating liquids into the flame.[23]
3. A variety of electrodeless discharge lamps,[24] and a 2450 megacycle, 125 watt rf power supply.[25]
4. A d.c. arc with a variety of metal electrodes.
5. A neon filled hollow cathode lamp, with cesium/aluminum cathode,[26] and its power supply.[27]
6. A rotating step sector disc[28] with step ratio 1.3 to 1.
7. A 3-step neutral density filter[29] with transmissions of 100%, 25%, and 6%.
8. A special 8-step slit, photochemically etched from steel shim stock, with log (step ratio) = 0.15.

A number of photomultiplier tubes and their associated amplifiers and power supplies are on hand, and a high speed (f/4) grating monochromator[30] can be used to monitor light intensities photoelectrically. A high speed electromechanical shutter is available that permits time-resolved photographic spectroscopy. Versions of this shutter are available that mount on the entrance slits of all spectrographs now on hand. Some details of shutter designs and operation are contained in references 31, 32, and 33. Electronic circuitry providing synchronization of shutter action with the compression cycle is described in reference 18.

Miscellaneous Accessories

All gas line connections are made with 3/8 inch dia. copper tubing and Swagelok fittings.[34] The high pressure valves[35] are designed to withstand 3000 psi continuous working pressure. The high pressure gas regulator[36] has a maximum inlet and delivery pressure of 2500 psi.

The project is equipped with complete facilities for quantitative spectrophotometry. A well-equipped darkroom with a temperature

regulated film processor[37] and a microdensitometer with strip chart recorder[38] permit measurements of relative intensities from the exposures on photographic plates and films.

IV. BALLISTIC ACTION TESTS

N_2 and CO_2

The first series of shots were made with N_2, and fired by slowly bleeding the plunger pressure, rather than by using the solenoid release valve. The first tests were limited to a few hundred atm maximum pressure (P_{max}) and no mechanical difficulty of any kind was experienced. Reproducibility of approximately 5% in P_{max} was obtained. When the solenoid valve was used to fire the piston, additional noise appeared in the outputs of the pressure gages mounted in the piston release section because of the more violent plunger motion, but it was found that P_{max} reproducibility was improved to better than 2%. A delay of approximately 20 milliseconds was found between the time the piston-actuated miniature switch in the piston release section opened and the time the gas pressure behind the piston rose to reservoir value. P_{max} data was obtained as a function of reservoir pressure (P_r) for piston masses of 1, 2, and 4 kilograms.

When fused quartz windows were installed in the end wall instead of the Kistler pressure gage, leaks were detected during both static vacuum and static pressure tests. Although test shots were made under these conditions, it was later found that by having the window mount sealing surface (a Poulter seal) polished to mirror finish and a flatness of less than 1 fringe the static pressure leaks were eliminated. No window damage was found during these initial tests.

During many of these early shots, recoil motion was monitored with the motion potentiometer and a typical maximum displacement of 1.6 cm was observed, when using a 2 kg piston at $P_{max} \approx 500$ atm. The maximum displacement was very closely synchronized with the time of maximum pressure. Figure 5 illustrates this synchronization and the ballistic action of the piston that results in multiple compressions. (Some ripple from a faulty CRO amplifier is evident in the pressure trace.)

Following these preliminary tests, further shots were made with both N_2 and CO_2 to test the compressor performance at higher pressures. With N_2, reservoir pressures up to 25 atm were used resulting in maximum pressures up to 2500 atm. With CO_2, reservoir pressures up to 18 atm yielded maximum pressures up to 2900 atm. These two series of shots were conducted with piston masses of 1, 2, and 4 kg for selected values of reservoir pressure in the N_2 series, and for 1 and 4 kg piston masses the CO_2 series. Each series of tests was halted when the maximum pressure rating (3000 atm) of the Kistler (model 607) pressure transducer was approached.

No mechanical trouble of any kind was experienced during these series of tests. In addition to measurements of peak pressure (P_{max}), the width of the pressure pulse at 1/2 P_{max} was measured for each shot, and also the "flight time" for the piston to go from rest to P_{max} was recorded. Shown in Fig. 6 are the curves of P_{max} vs. P_r for N_2 and CO_2 and for both 1 and 4 kg pistons, and for initial conditions in the test gas of NTP. Also shown are the ideal gas, isentropic curves for both diatomic ($\gamma = \frac{7}{5}$) and triatomic ($\gamma = \frac{9}{7}$) gases, calculated with assumption of no heat transfer to the walls, no mass leakage past the piston, no friction, and constant P_r during the compression cycle. Experimental data for N_2 are also shown which were obtained later in the program when a Kistler pressure gage (model 617A) with a maximum allowable pressure of 6500 atm was obtained.

Ar and He

Following the sucessful initial tests with N_2 and CO_2, the rare gases Ar and He were used as test gases. The use of these gases provided no new mechanical tests but did provide tests of the ability of the high pressure test section components to withstand high temperature conditions. Maximum pressures, flight times, pressure pulse half-widths, and recoil motion were all monitored as before, and the tests proceeded with no difficulties up to $P_{max} \approx 2100$ atm with Ar. The results of P_{max} vs. P_r for Ar and He are shown in Fig. 7, and data for pressure pulse half-widths and flight times are

shown in Figs. 8 and 9, and the corresponding results for N_2 and CO_2 are also shown.

Two problems appeared when He was tried as the test gas. The tests proceeded normally, as for N_2, CO_2 and Ar, until a value of P_r = 20 atm was tried with a 1 kg piston, and with the Kistler (Model 607) pressure gage in the end wall. At that pressure and with that piston, a very loud "screeching" noise was heard, no pressure pulse was detected and upon disassembly, the piston was found approximately 1/3 of the distance down the tube, and an unusually large quantity of copper dust was found in the tube, behind the piston. Inspection of the test section revealed no evidence that the piston had ever advanced that far during the shot. Subsequent tests, using heavier pistons with the same radial clearance between piston and tube, and 1 kg pistons with reduced radial clearance, as well as tests at other values of P_r with both Ar and He, resulted in normal, free-piston, ballistic action yielding expected values of P_{max}. It is presumed that the unusual performance was due to the existence of a condition which acted to destroy the pressure differential across the piston, the condition presumably being caused by a particular value of the gas leakage rate across the piston, because the leakage rate will be a function of radial clearance, pressure drop across the piston, piston velocity, and gas viscosity.

The second problem became apparent during the He test but later was found to exist with Ar as the test gas as well. This was the ablation problem mentioned earlier (see Cleaning Procedures), in which melting of the piston leading edge occurred, at the time of maximum compression, due to large heat transfer to the copper piston from the hot gas rushing through the annular space between piston and test section wall. The ablation was found experimentally to occur at lower calculated temperatures when He was used than was the case for Ar. The steps taken to eliminate piston ablation will be described in the Piston Materials Tests section of this report.

Tests with Variable P_o

Prior to optical tests and further materials testing, two more series of ballistic action tests were made. The first was a series of shots using Ar and He with the initial pressure in the tube, P_o, equal to 0.5 atm. This P_o was obtained by pumping down to less than 0.5 atm and slowly filling to the desired pressure. It was found that by reproducing P_o to within 1 mm Hg, P_{max} was reproduced to within 4%. The second series was made with P_o = 2.0 atm with both Ar and He, and the maximum pressures obtained for both P_o = 0.5 atm and P_o = 2.0 atm are shown in Fig. 7. The dashed line in that figure is an empirical relation that fits the observed data, for both He and Ar and for all the P_o values used, to within a mean error of $\pm$ 7% for a compression ratio range of 1.5 dex. No mechanical problems were experienced during any of these tests, but the final shot in the P_o = 0.5 atm series with He resulted in severe ablation of the piston and a thick deposit of Cu on the test section bore; the deposit had to be removed chemically with a warm bath of chromic acid.

The piston ablation was a serious limitation on the range of physical conditions which could be readily achieved with this compressor, and consequently the ablation problem was immediately attacked. The attack took the form of an extensive series of tests involving a number of refractory materials. These tests will be described in Chapt. VI.

Light Pistons and Shock Waves

Further ballistic action tests were made with pistons of a design slightly different from the initial, right-circular-cylindrical shape. The principal difference was a smaller diameter in the middle section with a short, full-diameter, bearing surface (with no grooves) at each end; the radial clearance at each bearing surface was the usual 45 micron clearance. A set of five identically dimensioned pistons were made. All were 5.0 cm long, but each was made of different material: phosphor-bronze, aluminum, magnesium, ATJ graphite, and nylon; the mass of each was 0.863 kg, 0.270 kg, 0.173 kg, 0.165 kg, and 0.111 kg, respectively. An additional set of 5 pistons, made of the same above

materials with the same masses, was made with radial clearances of 22 microns, but these pistons were not tested. All five pistons were tested with Ar and at identical initial conditions of P_o = 1.0 atm, P_r = 30.0 atm. Maximum pressures obtained are plotted as a function of piston mass in Fig. 10; data for heavier pistons from earlier tests are also shown.

A marked dependence of P_{max} on piston mass can be seen in Fig. 10 for piston masses less than 1 kg. An example of the Mg piston pressure vs. time record (the output of the Kistler pressure transducer displayed on a CRO and photographed with a Polaroid Land camera) is shown in Fig. 11 (a). Figure 11 also shows, for comparison, typical pressure records for Ar compression with a 4 kg piston, Fig. 11 (b), and a He compression with a 1 kg piston, Fig. 11 (c). The maximum pressures plotted in Fig. 10 were measured at the points of greatest pressure; there was no attempt made to find an average value of the pressure fluctuations.

The pressure fluctuations in the records and the dependence of P_{max} on piston mass can both be discussed in terms of shock wave formation. The finite speed of the piston generates hydrodynamic shocks in the test gas. These shocks run back and forth between the moving piston and the fixed end wall. The presence of these shocks causes the compression process to deviate from a reversible adiabatic process, even if heat transfer losses and mass leakage can be ignored. For purposes of discussion, the compression process can be considered to be one of two limiting cases. The first is one in which the irreversibilities induced in the test gas by the shocks may be considered negligible, and the second is the one in which the entropy increases associated with the shock waves cannot be neglected. The first case has frequently been used to calculate gas temperatures and densities achieved in this compressor and in earlier ones, although it is understood that the calculations yield only approximations to the actual gas conditions because of the idealized assumptions regarding friction, heat loss, and mass leakage across the piston. Pressure fluctuations indicating the presence of shock waves during the compression cycle was found to be small or absent over a wide range

of operating conditions, and the maximum pressures were found to be quite insensitive to piston speed. These two findings justified continued use of the isentropic compression relations for estimates of gas conditions because piston speed (or mass) did not enter into the relations between initial gas conditions and final, peak conditions. It should also be pointed out that the absence of shocks will minimize the inhomoqeneity of the compressed test gas and thus simplify both the gas diagnostics and the analysis of the spectral line shapes.

However, for piston masses less than about 1 kg, piston speed (or mass) is an important parameter for determining the gas conditions. There are a few treatments of shock formation accompanying isentropic compression in the literature. Evans and Evans[39] treat the case of a piston moving into a closed cylinder with constant speed after being suddenly accelerated from rest. The resulting shock is assumed to divide the test gas into two uniform regions, shocked and unshocked. The entropy of the gas increases as each shock passes, and the product PV^{γ} no longer remains constant but becomes a function of entropy. For isentropic compression, a plot of lot P vs. log V results in a straight line with a slope of $-\gamma$. Evans and Evans have shown that if shocks are also present, after a sufficient number of reflections have occured the possible values of P and V lie along another straight line parallel to the isentropic one but displaced upward from it such that compression to a given volume V results in a pressure P greater than the corresponding isentropic pressure. They further found that the greatest relative increase in the entropy function occurs in the passage of the first shock wave.

Further work on the problem of shocks accompanying isentropic compression has been done more recently by Minardi and Schwartz.[40] They have shown that there exists a critical value of a piston mass parameter, $\gamma W_p/W$, where γ is the ratio of specific heats of the test gas, W is the weight of the charge of test gas ahead of the piston, and W_p is the weight of the piston. For values of $\gamma W_p/W$ greater than the critical value, the peak pressure produced by a given reservoir driving pressure is not a function of $\gamma W_p/W$, but for values less than the critical value, peak pressures produced by a given driving

pressure fall off sharply with decreasing piston mass. Our results in Fig. 10 confirm the above relationship, but in order to calculate the critical value of the piston mass parameter using the treatment of reference 40, considerable computation and evaluation of frictional forces is required. However, the following physical argument based on the work of Evans and Evans[39] explains the reduced peak pressures obtained with decreasing piston mass.

In Fig. 12 we have drawn the conventional PV diagram mentioned above, but P, V, and T have all been plotted in units of their initial values, with the following notation:

$$\pi = \frac{P}{P_o}, \quad \tau = \frac{T}{T_o}, \quad d^{-1} = \frac{\rho_o}{\rho} = \frac{V}{V_o} = (\text{relative density})^{-1} \tag{1}$$

The line AB is the ideal isentropic relation in the PV-plane described by the equation:

$$\pi d^{-\gamma} = 1 \tag{2}$$

where γ is the ratio of specific heats for an ideal gas and has the value 5/3 in Fig. 12. The line AC is the corresponding line in TV-plane described by the relation:

$$\tau d^{1-\gamma} = 1 \tag{3}$$

The two lines AB and AC intersect at point A where $\pi = \tau = d = 1$, which are the initial conditions for the compression process. If shock waves are formed, Evans and Evans have shown, as mentioned above, that after a few reflections between end-wall and piston face the compression process will proceed along a pair of straight lines FD and FE parallel to AB and AC (shown dashed in Fig. 12) but displaced vertically from AB and AC by an amount ϵ corresponding to the limiting value of the change in the entropy function as the number of reflections becomes large. An actual process starting from point A will follow the dot-dash curves to the straight lines FE and FD.

For a given compression, for example to the line GCB, the maximum pressure and temperature achieved in the case of shocks being present will be greater than the isentropic values at B and C,

respectively. However, for a given initial pressure P_o for the test gas and a given reservoir driving pressure P_r, the increased pressure in the test gas due to shocks will result in a smaller pressure differential across the piston during the early compression stages. Consequently, this reduction in effective driving pressure will result in a smaller volume compression ratio. Therefore, a driving pressure that would result, for example, in achieving the compression ratio G in Fig. 12, and the points B and C in the absence of shocks, will, in the presence of shocks, yield a compression ratio to the right of the point G. If we now assume that the temperature of the compressed gas is proportional to its internal energy, which in turn is proportional to the work done on it by the piston, then the point C must be the upper limit for the gas temperature achieved with the initial operating conditions regardless of whether or not shocks are formed. If shocks are formed, the point D must then correspond to the maximum compression ratio that can be achieved, and the maximum pressure will then be that at point E. The pressure for point E will always be less than for point B because of the equal vertical separations between solid and dashed curves and because the τ_d curves have smaller slopes than the π_d curves. The dashed curves in Fig. 12 were drawn using the calculations of Evans and Evans for an initial shock strength $\sigma_1 = (P_1/P_o) = 5$, where P_1/P_o is the pressure ratio across the first shock wave before reflection from the end-wall. If the initial shock strength were greater than 5, i.e., a lighter piston and the same initial driving pressure, the dashed curves would be displaced further upward, the intersection at D would move to D' and the intersection point E' would occur at a still lower value of π relative to that for point B. This variation of P_{max} with piston mass is the behavior displayed in Fig. 10.

V. HIGH PRESSURES AND TEMPERATURES

Brief mention has been made earlier in this report of achieving the 5000 atm pressure limit of the test section (see Fig. 6), and of the ablation problem encountered when He and Ar were compressed. In the following section we discuss those experiments more fully, and discuss pressure gage and window tests. All gas temperatures quoted in this section, as well as throughout this report are estimates of the real translational temperature based on the results of the temperature diagnostic scheme described in reference 11. In that work, most of which was done with helium as the test gas, it was found that the peak gas temperature was related to the maximum gas pressure by an equation of the ideal, isentropic form but containing a polytropic exponent 6% smaller than the adiabatic exponent 1.667:

$$(T_{max}/T_o) = (P_{max}/P_o)^{1.572}$$

This relation yields temperatures roughly 25% less than the adiabatic temperature in the 3000°-6000°K range, and this correction factor has also been applied in estimating N_2 temperatures quoted in this report.

Piston Materials Tests

Even before attempts were made to achieve the pressure design limit of the high pressure test section, it became clear that the piston ablation problem, if unsolved, presented a severe limitation on the operating range of this compressor. The attack on this problem took two forms. First, attempts were made to fasten refractory materials to the face of the piston, and second, a simultaneous study was made to determine the feasibility of inserting a refractory liner material into the bore of the test section.

The refractory materials chosen for piston head experiments were graphite, boron nitride, molybdenum, and tungsten. Attempts to fasten disks of graphite to the phosphor bronze piston face with a special graphite bonding epoxy resin, as well as with Eastman "910" brand cement, failed, and consequently heads of the above refractory

materials were made to fit a specially designed piston containing a threaded axial hole for a retaining screw. A photograph of the disassembled piston and a graphite head is shown in Fig. 13. It was found that with the relatively weak materials, such as graphite and boron nitride, the diameter of the retaining screw head must be minimized to prevent the screw from crushing and fracturing the material. There was no difficulty encountered in the use of the refractory metals. Their fabrication, however, was difficult and costly.

All the above materials were tested with Ar at temperatures up to approximately 6000°K. The results are summarized as follows:

Graphite- Heads of thickness greater than 3 cm prevented piston erosion. The heads decreased in diameter approximately 10-15 microns per shot, and small quantities of graphite powder became mixed with the test gas resulting in increased continuous intensity in the emitted spectra.

Boron nitride- Surface decomposition occurred at temperatures greater than 4000°K.

Molybdenum- Slight discoloration occurred at leading edges at the highest temperatures tested; otherwise, no substantial defects were detected.

Tungsten- Performed in a similar manner as molybdenum, except that a small chip broke off the leading edge in its final test and it was not tested further. The molybdenum piston head is being used routinely now for all experiments involving rare gas compression.

Test Section Bore Materials

The second part of the problem, protection of the test section bore from thermal degradation, has been solved only to the extent that it has been shown to be mechanically feasible to insert a molybdenum or tantalum liner into the test section. The study of the problem has shown that it is necessary to choose the OD of the liner greater than the ID of the bore by approximately 50 microns for 4.7 mm thick Mo liner. This amount of interference will result

in the liner remaining with its elastic limit in compression without internal gas pressure and yet its elastic limit in tension will not be exceeded when the internal gas pressure is less than 5000 atm. However, the exact amount of interference to be chosen is critically sensitive to the values of tensile, shear, and compressive strengths, Young's moduli, and Poisson's ratios of both liner material and its steel casing. In view of the variations of these quantities in commercial products, it was deemed the wiser course to be content with the performance of the 25 micron coating of electroplated chromium which has been applied to the bores of all test sections on hand, and which have survived with negligible damage repeated shots of temperatures up to 6000°K. Further work on refractory liners will await the desire to exceed that gas temperature.

Pressure Gage Tests

A variety of transducers have been used to measure test gas pressures as a function of time during the compression cycle. These devices and their evaluations are described below in the chronological order in which they were obtained.

NOL Gages- These gages were designed and made for the work done on the original NOL compressor (see references 41 and 42 for descriptions of their design, construction, and performance). They are quartz crystal gages cemented to a flexible diaphragm. An end-plug adaptor for them was made, and their performance was found to be quite satisfactory. Their response time was adequate to reveal the pressure fluctuation due to shocks, and they displayed acceptably low noise levels. Their use was restricted to pressure below 2000 atm because of the lack of calibration facilities at higher pressures, and the method of sealing them into the adaptor to prevent gas leakage rendered them difficult to interchange and inconvenient for general usage.

Kistler, Model 607- This is a commercial, quartz crystal transducer. It is similar to the current Kistler Model 607B. It has a nominal pressure capacity of 2000 atm but can be safely overloaded to 3000 atm. This gage is exceptionally noise free, and has

given trouble free service over a wide range of compressor operating conditions. It has been dynamically calibrated in this laboratory up to 2000 atm, and the calibration has been linearly extrapolated to 3000 atm.

Kistler Model 605B/633B- This gage is a low pressure transducer (605B) mounted in an adapter (633B) containing a small, step-down piston bearing against the 605B diaphragm in such a way that the pressure exerted on the diaphragm is less than the gas pressure. With the 605B/633B combination, the maximum pressure measured can be as high as 10,000 atm.

It was hoped that with this gage we could attempt to reach the 5000 atm design limit of the test section. However, it soon became clear that this gage was unsuitable for use in this compressor. The amplitude of the noise was very nearly the same magnitude as the pressure signal. The noise was not of the underdamped ringing type of noise often experienced in transient pressure measurements, but rather had a random character which was presumed to be due to a combination of effects from disturbances in both the compressed gas and the test section itself (such as mechanical vibrations). The essential defect of this gage is thought to be the relatively unrestrained step-down piston which can rather easily be set into motion by shocks or vibrations thus generating noise signals.

Kistler 617A- When the Kistler Instrument Corporation was informed of the above difficulties, they suggested we try an experimental version of a gage then under development by them. This gage was called Model 617A, but is now in production in modified form as the Model 607B. The 617A is rated for 5000 atm, but can safely be overloaded to 6300 atm.

The performance of this gage was found to be very acceptable, it being only slightly more noisy than the 607. The noise is most likely due to the two-piece construction in which a separate conical sealing ring is used to eliminate side pressure on the gage body.

The calibration supplied by Kistler has been used, and small discrepancies between this gage and the Model 607 begin to appear at approximately 1000 atm.

Using this gage and the Kistler calibration, we have succeeded in compressing N_2 to a peak pressure of 5000 atm, starting with initial pressure of both 1 atm and 0.5 atm. The only problem experienced was the difficulty encountered in disconnecting the tube from the piston release section after exceeding 3500 atm. The difficulty was traced to a deformation of the piston release section at the threaded portion which mates with the rear coupling nut. This section experienced an unexpectedly high tensile stress during moments of peak compression. The problem was solved by modifying the piston release section design and inserting a specially hardened section mating with the coupling nut. After accomplishing this modification, 5000 atm peak pressure was readily achieved.

WINDOW TESTS

There is a wide variety of windows available for use in this compressor, and all of the principal varieties have been tested to determine optimum design features, upper limits of working pressure, and probable causes of failure. The principal window material used has been "schlieren quality" fused silica, free from bubbles and striations. Other materials tested have been a borosilicate Corning glass and clear synthetic sapphire.

The windows are all right circular cylinders. The side surfaces are unpolished, and the flat end faces are usually polished flat to less than 1/2 fringe. The edges are usually beveled slightly for stress relief. The windows are mounted in a loose fitting cap with a small lip which extends slightly over the face in contact with the test gas. This lip serves only to prevent the window from being pulled into the test section during vacuum operations. The outside face of the windows contacts the optically flat (1/2 fringe) surface of the window mount. The compressed gas pressure forces the two flat surfaces together to form a "Poulter" seal. A 1 cm diameter hole in the flat window mount surface constitutes the viewing port.

The window mount is sealed into the test section with a conventional Bridgman seal (see Fig. 3).

The upper limits of working pressure are functions of both material and thickness. The limits for use in the compressor are summarized in the following table:

Material	Thickness (mm)	Pressure Limit (atm)
Fused silica	19	3000
Fused silica	13	2000
Corning glass	13	2000
Sapphire	13	5000

This table contains data only for windows mounted centrally in the end-wall. Somewhat different and more erratic performance is obtained from windows mounted in side-window test sections (see section VI), due presumably to unsymmetrical loading conditions.

The characteristic mode of failure is a symmetrical pattern of small cracks and chips at the unsupported area of the outer face, the interface between window and ambient room air. A roughly hemispherical volume, with diameter equal to that of the viewing port, fractures into tiny chips which usually fall out into the exit viewing tube. Occasionally, upon severe overload conditions, radial cracks can be seen directed outward toward the circumference from the unsupported area. Some examples of these failures are shown in Fig. 14 in which also is shown a lucite window which was unintentionally overloaded to the point where a hole was blown completely through the window.

It is presumed that the mechanism giving rise to the hemispherical fractures is a reflection of the outgoing compression wave at the fused silica-ambient air interface which gives rise to a tension wave reflected back into the fused silica. The amplitude of the reflected tension wave increases as the difference between the characteristic impedance of the two media increases[43]:

$$A_{refl} = A_{incident} \left[(\rho c)_a - (\rho c)_q\right] / \left[(\rho c)_a + (\rho c)_q\right] ,$$

where $(\rho c)_a$ and $(\rho c)_q$ are the characteristic impedances (products of density and sound speed) of air and fused silica respectively, and where A_{refl} is the reflected tension wave amplitude and $A_{incident}$ is the amplitude of the compression wave normally incident at the interface. Since

$$\frac{(\rho c)_q}{(\rho c)_a} \approx 4 \times 10^4$$

then

$$\frac{A_{refl}}{A_{incident}} \approx 1 \quad .$$

In view of the weakness of glasses and fused silica in tension relative to their compressive strength, the above mechanism is felt to play an important role in window failure in this compressor.

Synthetic sapphire has not exhibited the above failure in 13 mm thick samples up to 5000 atm, and consequently is used routinely now for nearly all radiation studies and spectroscopic experiments that exceed 3000 atm.

VI. RECENT COMPRESSOR MODIFICATIONS

SIDE-WINDOW TEST-SECTIONS

The initial design of the high pressure test sections (see Fig. 3) permitted optical measurements through the end-plug, or pressure measurements via a quartz crystal transducer in the end-plug, but not both measurements simultaneously. It soon became apparent that simultaneous pressure and spectroscopic temperature measurements were required for diagnostic purposes, and that absorption spectroscopy experiments would be necessary to solve certain atomic physics problems. Consequently, more versatile test-section configurations were designed for these experiments.

The first such design permitted the insertion of two diametrically opposed side-windows. The details of the design are shown in Fig. 15. The window sealing techniques use the same Poulter and Bridgman seal principles as described in section V. The window jackets have a cylindrical end surface to match the test-section bore and alignment keys to prevent jacket rotation. The inner window surface is nearly tangent to the cylindrical bore to yield a 5 cm. optical path between windows. The windows are located in a thick-walled portion of the test-section near the normal end-wall location. The end-wall location is chosen such that the side-window axis will be midway between the end-wall and the expected piston position at maximum compression.

This two-window test-section was originally designed for a gas density measurement experiment. In that experiment, the windows were not jacketed and had concave cylindrical inner faces, thus forming an optical system consisting of two negative cylindrical quartz lenses (the windows), and a positive cylindrical gas lens with a focal length varying inversely with the refractivity of the test gas. The defocussing of a light beam passing through this lens system provided an analogue signal which, with a suitable calibration, yielded a gas density via the Lorentz-Lorenz law. Preliminary trials indicated that this scheme was feasible, but that large error signals were

produced by small vibrations in some of the optics external to the test-section, and that further errors were present due to partial absorption of the transmitted beam in what was erroneously thought to be an optically thin continuum. These experiments were discontinued, and diagnostic efforts were diverted to spectroscopic temperature measurements from which the gas density is calculated with acceptable accuracy via the ideal gas equation of state (references 10 and 11).

Improvements in the side-window configuration were incorporated in the design of a 4-port test-section. This test-section, with two pairs of diametrically opposed windows in the same plane normal to the test-section axis, allows simultaneous emission and absorption experiments, or, with the aid of external mirrors, allows multiple pass absorption experiments to be performed. This design, shown in Fig. 16, is somewhat simpler to fabricate than the 2-port test-section, and employs the same Bridgman and Poulter seals as the earlier window mounts. Note that the chamfered window cap with the separate key to prevent rotation in Fig. 15 has been replaced in Fig. 16 with the straight cylindrical jacket and integral alignment pin. Both side-window test-sections use identical window sizes, window mounts, Bridgman seal components and seal compression nuts, and solid plug adaptors and Kistler pressure gage adaptors are available for each test-section. The bores and concave surfaces of the window jackets are electroplated with a flash coating of copper, and an overcoating of approximately .001" thickness of chromium. All radial clearances and tolerances are held generally to $\pm$.0005" to minimize ablation damage around the window jackets.

The performance of both test sections has been satisfactory in terms of minimal window breakage, although the 4-port section is slightly superior in this regard. Both sections suffer rapid deterioration of the chromium coating on shots that achieve gas temperatures exceeding 6000K. The solution of this problem awaits a feasible refractory metal liner design.

Minimum Separation Gages

It is frequently necessary to know accurately the minimum piston/end-plug separation. This information permits calculation of the minimum volume of the test gas, and, in addition, on diagnostic shots based on the attenuation of a test beam by the test gas, prevents errors caused by partial blockage of the test beam by the piston at the end of the compression stroke. A telescopic minimum separation gage was designed and constructed. It consists of two concentric interference-fit tubes. The outer tube is a solid thick-walled tube threaded on one end for attachment to the face of the end-plug. The inner tube is thin-walled and contains a slot along its length. One end is chamfered to facilitate insertion. Partial insertion of the inner tube into the outer tube is made prior to a shot. When the compressor is fired the motion of the piston forces the slotted inner tube into the outer tube to an extent determined by the closest approach of the piston to the end-plug. The minimum separation gage installed in the end-plug is illustrated in Fig. 17. Its use neither interferes with pressure and measurements nor with the recording emission or absorption spectra. The minimum piston/end-plug separation is determined by removing the end-plug from the high pressure section and measuring the distance from the end-plug face to the tip of the slotted inner part. The minimum separation gage can be reused by unscrewing the outer part from the end-plug, driving the inner part completely through the outer part, reinserting the inner part into the outer part (up to its predetermined initial position), screwing the assembled gage back into the end-plug face, and reinstalling the end-plug into the high pressure section.

The outer part of the gage is made of class O1 tool steel and is hardened to R_c50. Its inner diameter is honed to 0.353cm $\pm$ 8μ. The inner part is made of 4130 alloy steel tubing and has a 0.25mm wide slot along its entire length. An interference of 40-80μ gives a fit sufficiently tight to prevent overshooting (insertion of the inner part deeper than that caused by the motion of the piston), while at the same time not so tight as to interfere with the ballistic action of the compressor. No benefit accrues from

heat-treating the slotted inner part. A specially made dead-weight tester jig is available for checking the fit of the inner and outer parts of the separation gage, making the initial insertion, and for driving the inner piece through (out of) the outer piece after the gage has been used. A set of three outer part/inner part combinations covers the range from 5 to 62 mm in increments of 5-18, 15-36, and 30-62 millimeters.

Piston Seals

Leakage of reservoir gas across the piston during the acceleration part of the compression stroke, and leakage of test gas across the piston during the deceleration part of the compression stroke results in the following detrimental effects: 1) inability to predict accurately the ballistic action of the compressor, 2) inaccuracies in physical property measurements due to poorly known composition and quantity of test gas, and 3) oblation of piston and high pressure section surfaces that experience high heat transfer. Gas leakage can be reduced up to a point by reducing the clearance between the bearing surfaces of the piston and the bore of the compressor tube. A relatively soft metal possessing good wear qualities should be used as the piston bearing material (i.e. phosphor-bronze), and the compressor bore should be made of highly polished, hardened steel. Clearances smaller than approximately 0.001" (radial) result in excessive wear of the bearing surfaces and occasionally cause piston jamming.

Further improvement in leakage reduction can be made through the use of flexible, tight-fitting seals. Single and double cup-type seals (Fig. 18) were designed and fabricated of Teflon. The diameter of the bearing surfaces of the seals is made approximately equal to the bore diameter of the tube. Assembly is made with the open-end of each seal facing the gas that is being sealed. Figure 18 illustrates the seal assembly that attaches to the rear of the piston. The piston body is sufficiently long that even at minimum test gas volume the seals do not cross the test section-tube junction. The serrated ring and bolt-head visible in Fig. 18 provide support for

the cup-seal lips but also allow gas passage into the cups. When the double seals are used they are assembled with the cups back-to-back. As the compressor is fired the reservoir gas impinges on the rear of the piston and the rear cup is forced to expand radially reducing the clearance with the tube bore essentially to zero and thereby producing an effective gas seal. Near the end of the compression stroke, when the pressure differential across the piston reverses, the forward seal is actuated in a similar manner. Static tests with and without the cup-seals indicated a 100 fold reduction in leakage rate when the seals are used. A filled - Teflon material called RULON LD[44] with substantially superior wear properties is now being used in place of Teflon in order to increase the life of the cup-seals. The seals have been used up to a maximum dynamic pressure of 2500 atmospheres without failure.

Operations Requiring High Purity Test Gases

Spectral line broadening studies do not require the use of ultra-high purity test gases. The contaminants that most disturb those studies are metal vapors generated in the compression cycle that produce spectral lines that blend and interfere with the lines under study. One needs only to be confident that the test gas is sufficiently pure to constitute the principal collision partner for the metal atoms radiating the lines being studied.

The above requirement is unfortuanately not true for continuum spectroscopy. For such experiments, it is usually quite impossible to identify and determine the relative contributions of the several continuum emitting species in the test gas because nearly all continuum emission processes yield spectra with very weak wavelength dependence. Several common continuum emission processes have large emission coefficients, and consequently the chemical composition of the test gas must usually be determined to a much higher level of accuracy than is the case for line broadening studies. In order to identify weak continuum emission processes or to discover unusual continua that may be important only under the extreme conditions of temperature and pressure generated in the compressor, undesirable

contaminant species in the test gas must generally be present in amounts of 10 ppm or less. The present inability of the compressor and gas handling systems to achieve this level of purity has complicated our attempts to identify and measure the absorption coefficient of the quasi-molecular hydrogen association in the vacuum-ultraviolet spectral region (references 10 and 45).

The following improvements and procedures have been incorporated into the compressor facility to minimize contamination of the test gas.

(a) All reinforced butyl rubber hose connections have been replaced with copper tubing and Swagelok fittings. Teflon tape is used for pipe thread sealant. See Fig. 19 for the normal gas supply plumbing diagram.

(b) Low vapor pressure silicone vacuum grease is used for O-ring lubricant, and Viton-A O-rings used wherever possilbe.

(c) Gas regulators with metal diaphragms have been installed in all gas handling systems.

(d) Sintered bronze disk filters are installed near the inlets to the tube and test-section. These filters remove dust particles larger than 10 microns.

(e) No lubrication is used on the piston, tube, bore, or test-section assembly.

Vacuum procedure consists of pumping simultaneously on the tube and test section and the volume between the piston and plunger. (The pressure in that latter volume must always be equal to or less than the tube pressure to prevent premature piston motion.) A diagram of the vacuum and gas handling system which optimizes pumping speed and gas purity is shown in Fig. 20. Some compromises in pumping speed were required in order to retain a high pressure capability. The vacuum pump is a Welch Model 1402, 2 stage mechanical pump. The lowest pressure attainable in the test section and tube with this system is 5 microns, and the leakage rate is such that after pump shut-off and rapid filling with research grade test gas to

atmospheric pressure the impurity level is approximately 50 ppm, consisting chiefly of air leaking in during the filling operation. Some impurity gases are also adsorbed on the inner walls of the tube and test section, and on the piston, so that the final impurity content of the test gas at the peak of the compression cycle may be more than 100 ppm, even when using research grade test gases.

Two major undertakings are required to lower the test gas impurity level. The test-sections were designed primarily to seal against high internal pressure. For high vacuum operations they must be redesigned with good vacuum seals as well. Pumping speed may also need to be increased. The second major modification required is an ability to bake the tube, test-section and piston to remove adsorbed gases. This capability will also extend dramatically the operating ranges in density and temperature over which spectroscopic experiments can be performed and thus increase even further the versatility of the NOL ballistic piston compressor.

REFERENCES

1. G. T. Lalos, "Laboratory Production of Hot, Dense Gases", Rev. Sci. Instr. 33, 214 (1962).

2. D. Price and G. T. Lalos, "Adiabatic Compressor for Dynamic P-V-T measurements on Gases to 100,000 psi", Ind. Eng. Chem. 49, 1987 (1957).

3. G. T. Lalos, "The 10,000 Atm. Ballistic Piston Compressor, I. Design and Construction", NOLTR 63-96 (1963).

4. Automatic Switch Co., Florham Park, N. J.; model 82233.

5. Sunnen Products Co., St. Louis, Mo.; Portahone P-28.

6. G. T. Lalos and G. L. Hammond, Bull. Am. Phys. Soc. 7, 458 (1962).

7. G. L. Hammond and G. T. Lalos, Bull. Am. Phys. Soc. 7, 458 (1962).

8. G. L. Hammond, "Thermal Emission from the NOL Adiabatic Compressor", NAVWEPS Report 7369 (1961).

9. G. T. Lalos and G. L. Hammond, "Opacity of Hot, Highly Compressed Hydrogen", NOLTR 66-202 (1966).

10. G. T. Lalos and G. L. Hammond, "Gas Opacity Measurements with a Ballistic Piston Compressor", NOLTR 70-15 (1969).

11. G. L. Hammond, "Spectroscopic Temperature Measurements in Hot, Dense Gases", NOLTR (in preparation).

12. K. W. Reed "Spectroscopic Gas Mixture Analyzer", unpublished.

13. Clark and Wheeler, Inc., 16455 Minnesota Ave., Paramount, California.

14. Wallace & Tiernan, Inc., Bellville, N. J.; model FA-129160.

15. Heise Bourdon Tube Co., Newtown, Conn.

16. Dynamic Instrument Co., Cambridge, Mass.

17. Kistler Instrument Corp., Redmond, Wash.

18. H. Cleaver, "Digital Logic Circuits for Sequencing and Signal Displays for the NOL Compressor", NOLTR (in preparation).

19. Bourns, Inc., Instrument Div., Riverside, Calif.

20. Baldwin-Lima-Hamilton Corp., Waltam, Mass., type C-14.

21. Conax Corporation, Buffalo, N. Y.

22. Mole-Richardson Co., Hollywood, Calif., type 2371.

23. Beckman/Scientific Instruments Div., Fullerton, Calif.; model 9200 Flame Photometry Attachment.

24. Ophthos Instrument Co., Rockville, Md.

25. Baird-Atomic Co., Cambridge, Mass.; model NM-1.

26. Westinghouse Electric Corp., Elmira, N. Y.; type WL-22823.

27. Kepko, Inc. Flushing, N. Y.; model ABC-425.

28. Bausch and Lomb Optical Co., Rochester, N. Y.

29. Bausch and Lomb Optical Co., Rochester, N. Y., cat. #33-83-07.

30. Engis Equipment Co., Chicago, Ill.; model S05-02

31. P. A. Kendall, "A High Speed Electromechanical Shutter", NAVWEPS Report 7362 (1961).

32. P. A. Kendall, Applied Spectroscopy 18, 33 (1964).

33. P. A. Kendall, Applied Spectroscopy 22, 274 (1968).

34. Crawford Fitting Co., Cleveland, Ohio.

35. Whitey Co., Oakland, California.

36. Victor Equipment Co., San Francisco, Califronia; model GD 30-250.

37. Jarrell-Ash Co., Waltham, Mass., Model 34100.

38. Leeds and Northrup Co., Philadelphia, Pa.; cat. #6700-A1.

39. C. Evans and F. Evans, J. Fluid Mech. 1, 399 (1956).

40. J. Minardi and R. Schwartz, Aerospace Research Laboratories Report ARL 63-167, Wright-Patterson AFB, Ohio, 1963.

41. P. L. Edwards, "A High-Speed, High Pressure Gage", NavOrd Rpt. 2380 (1952).

42. P. L. Edwards, "A High-Speed, High Pressure Gage, Part II", NavOrd Rpt. 3963 (1955).

43. H. Kolsky, "Stress Waves in Solids", Dover Publications, New York, 1963, p. 34.

44. Dixon Corporation, Bristol, Rhode Island.

45. R. Doyle, Astrophys. J. 153, 987 (1968).

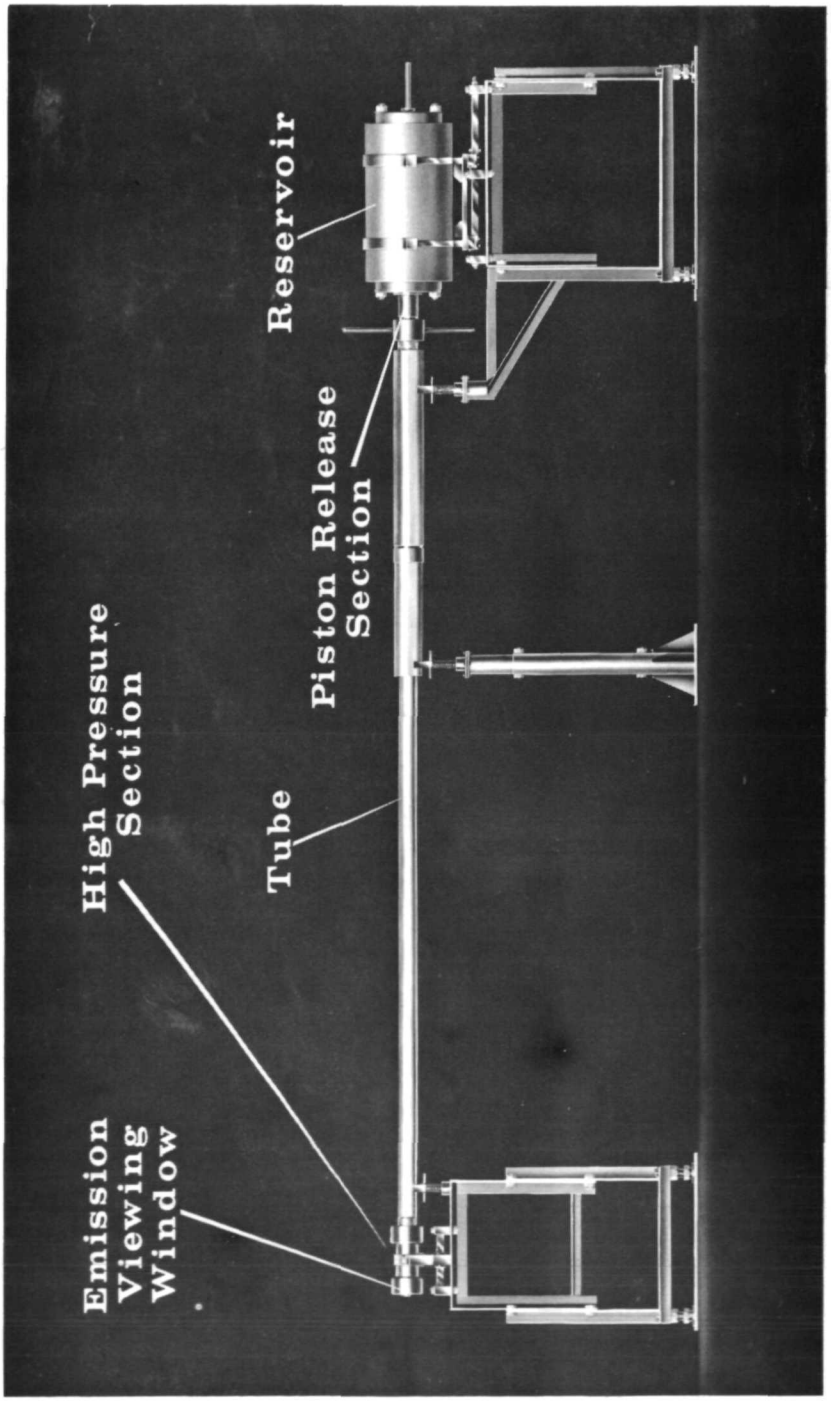

FIG. 1 BALLISTIC PISTON COMPRESSOR WITH 4 METER TUBE

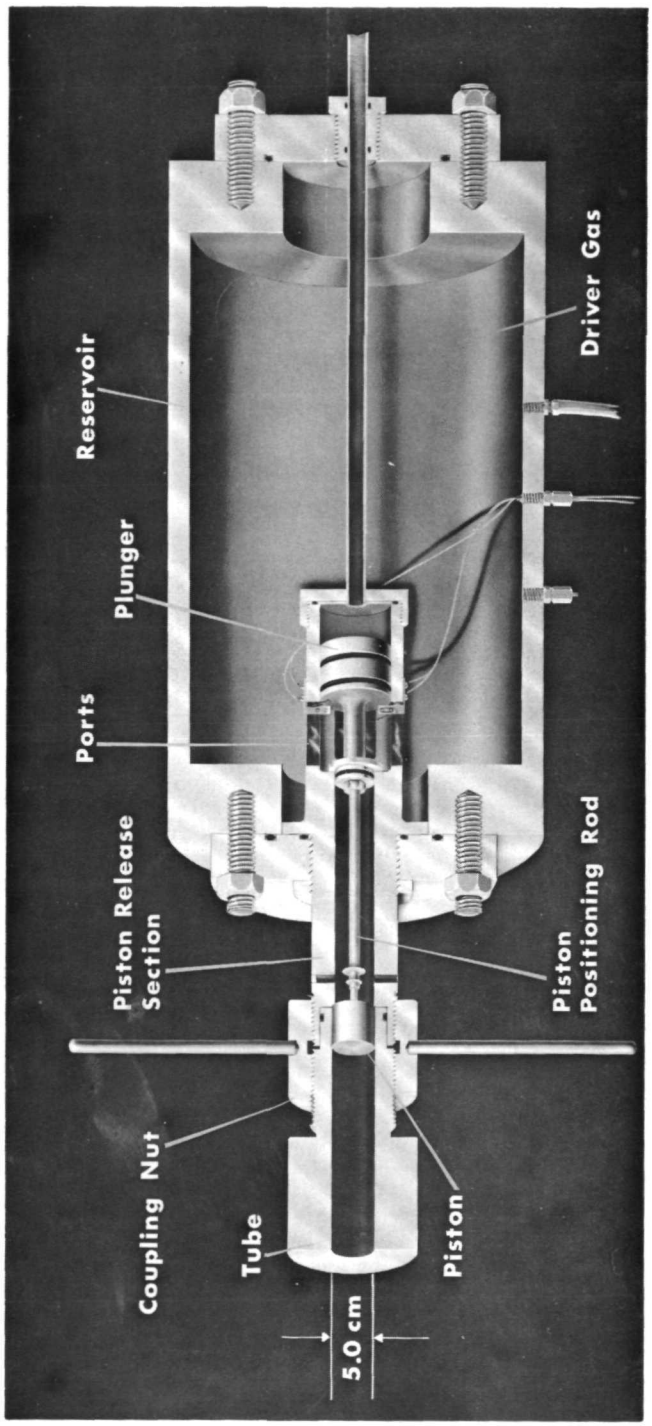

FIG. 2 DETAILS OF COMPRESSOR RESERVOIR AND PISTON RELEASE SECTION

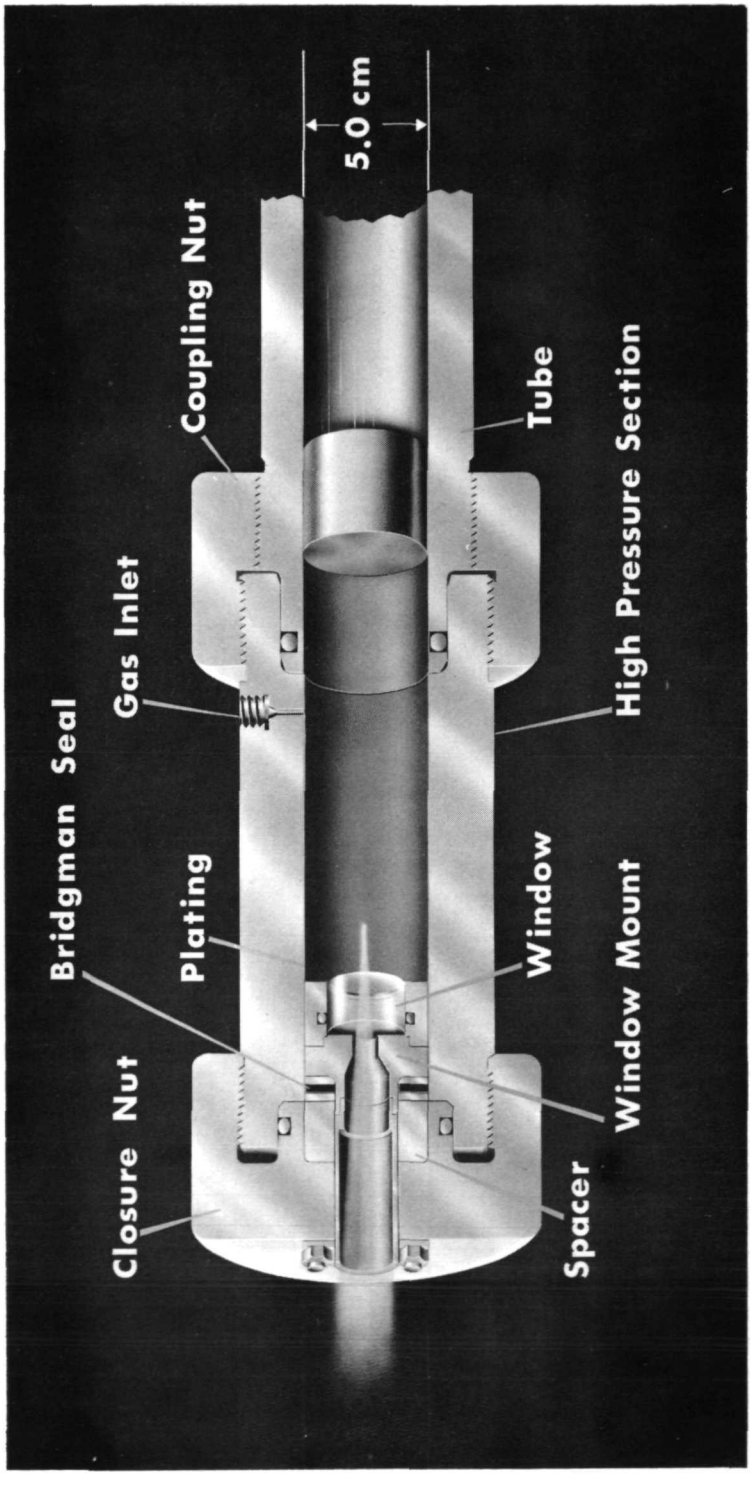

FIG. 3 INITIAL HIGH PRESSURE SECTION ASSEMBLY

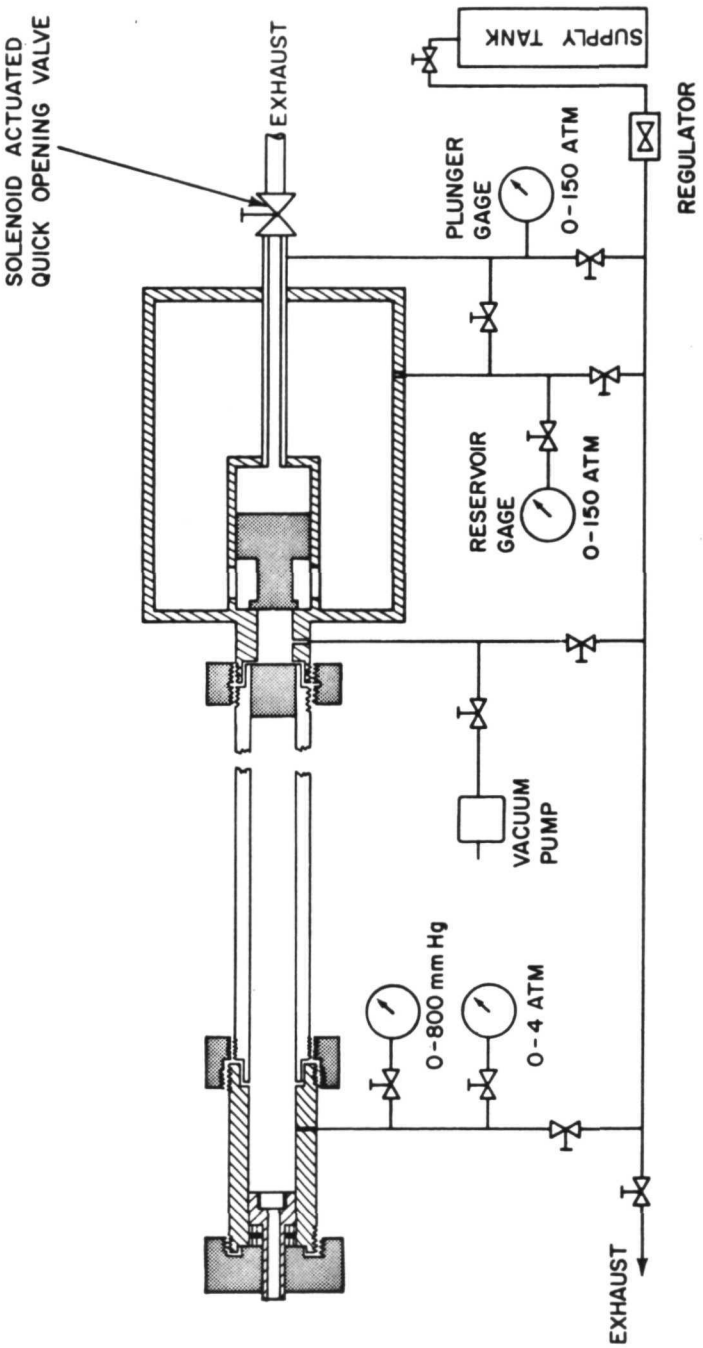

FIG. 4 GAS LINE SCHEMATIC DIAGRAM

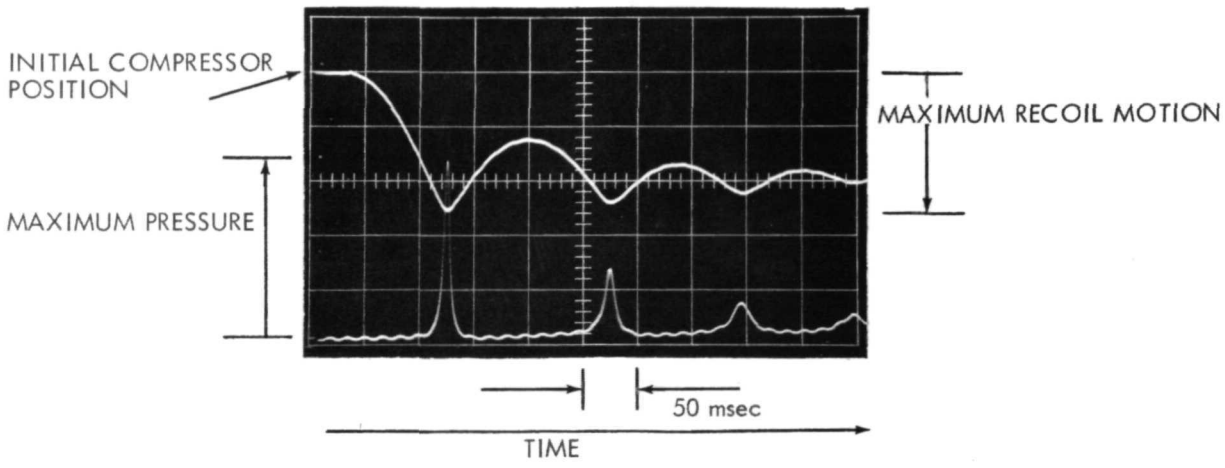

FIG. 5 PRESSURE AND MOTION RECORD
(a) UPPER TRACE: MOTION POTENTIOMETER, 1 DIV. = 6.3 mm DISPLACEMENT
(b) LOWER TRACE: PRESSURE TRANSDUCER, 1 DIV. = 70 ATMOSPHERES

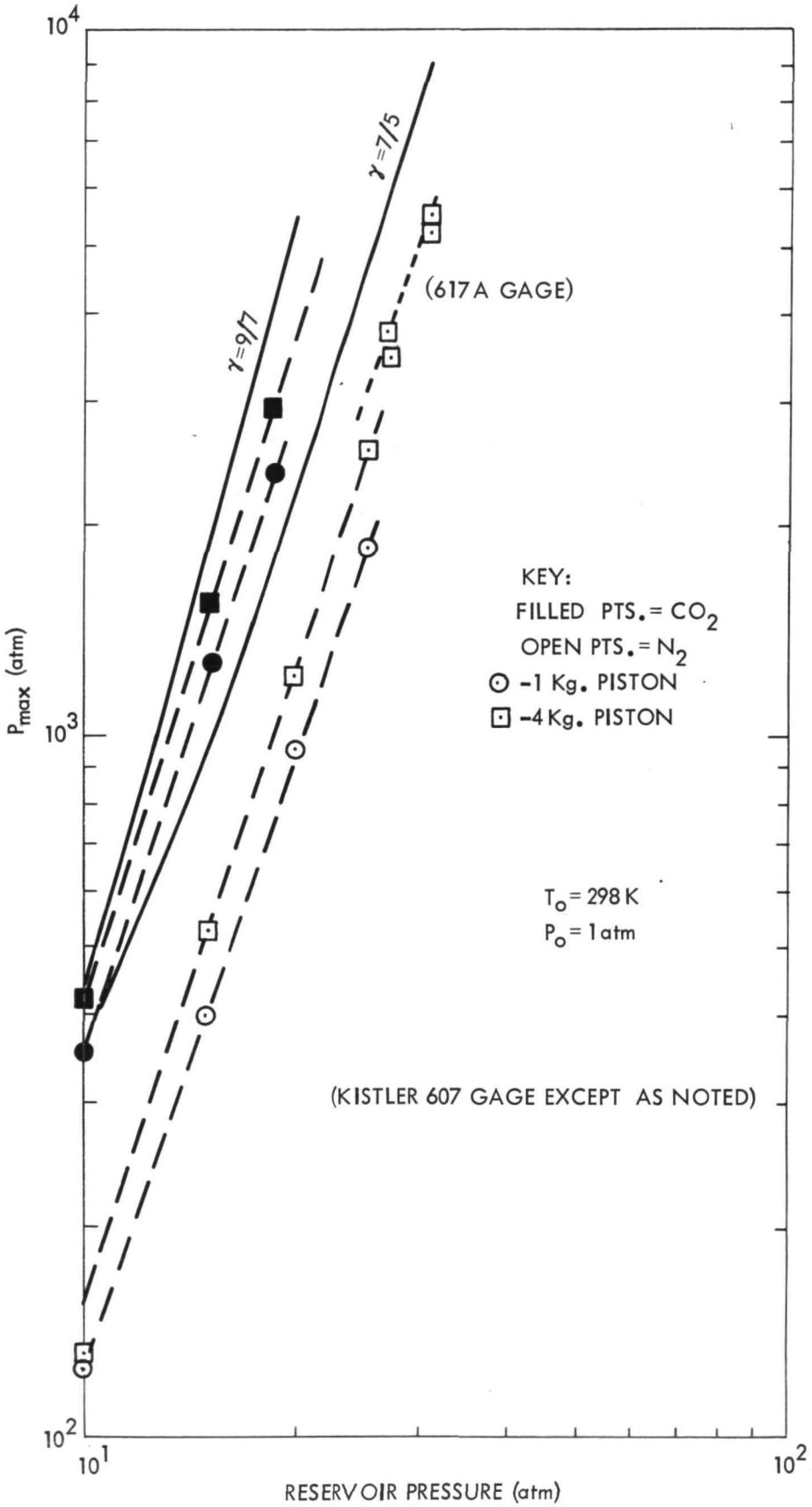

FIG. 6 MAXIMUM PRESSURE VS. RESERVOIR PRESSURE: N_2 AND CO_2

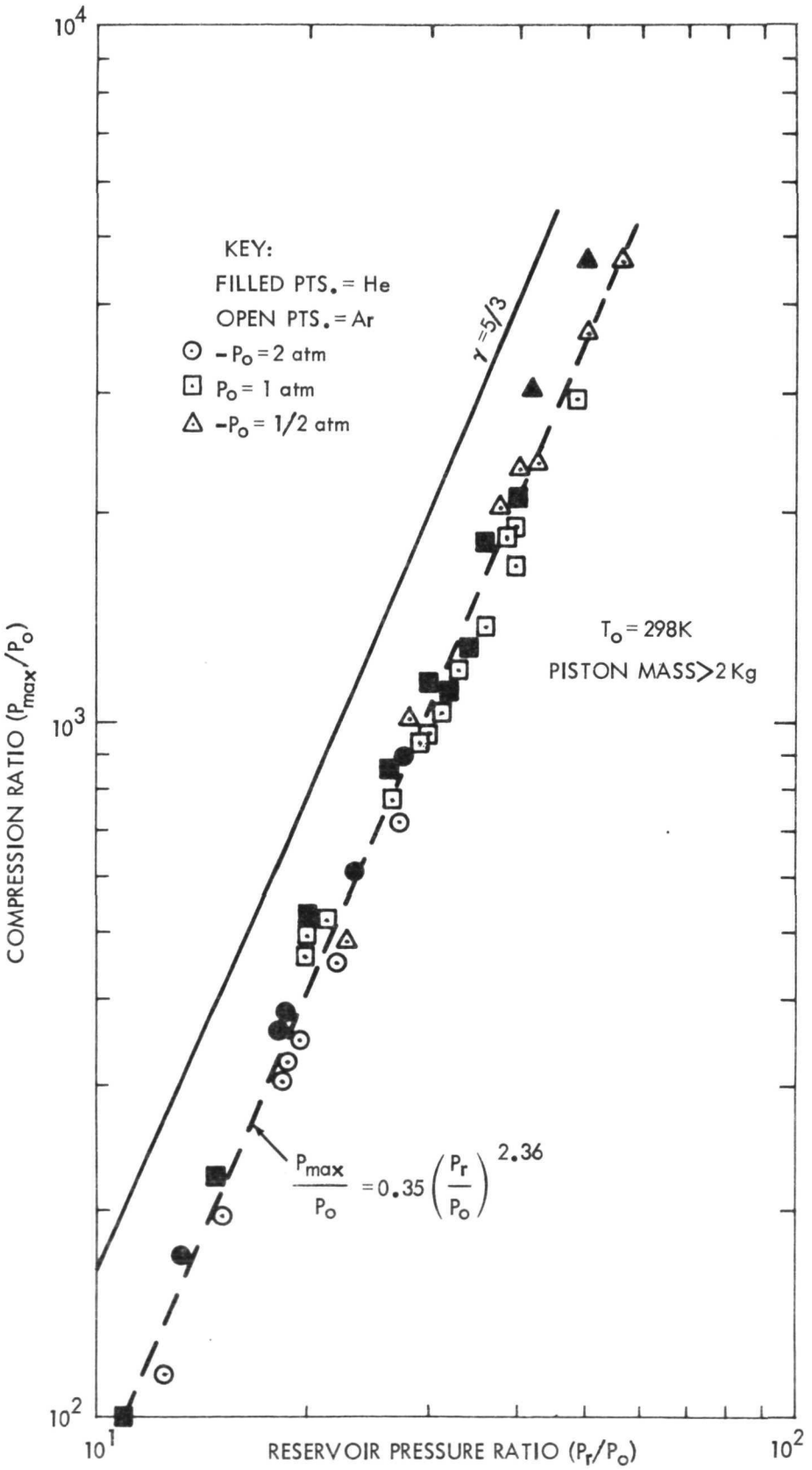

FIG. 7 MAXIMUM PRESSURE VS. RESERVOIR PRESSURE: Ar AND He

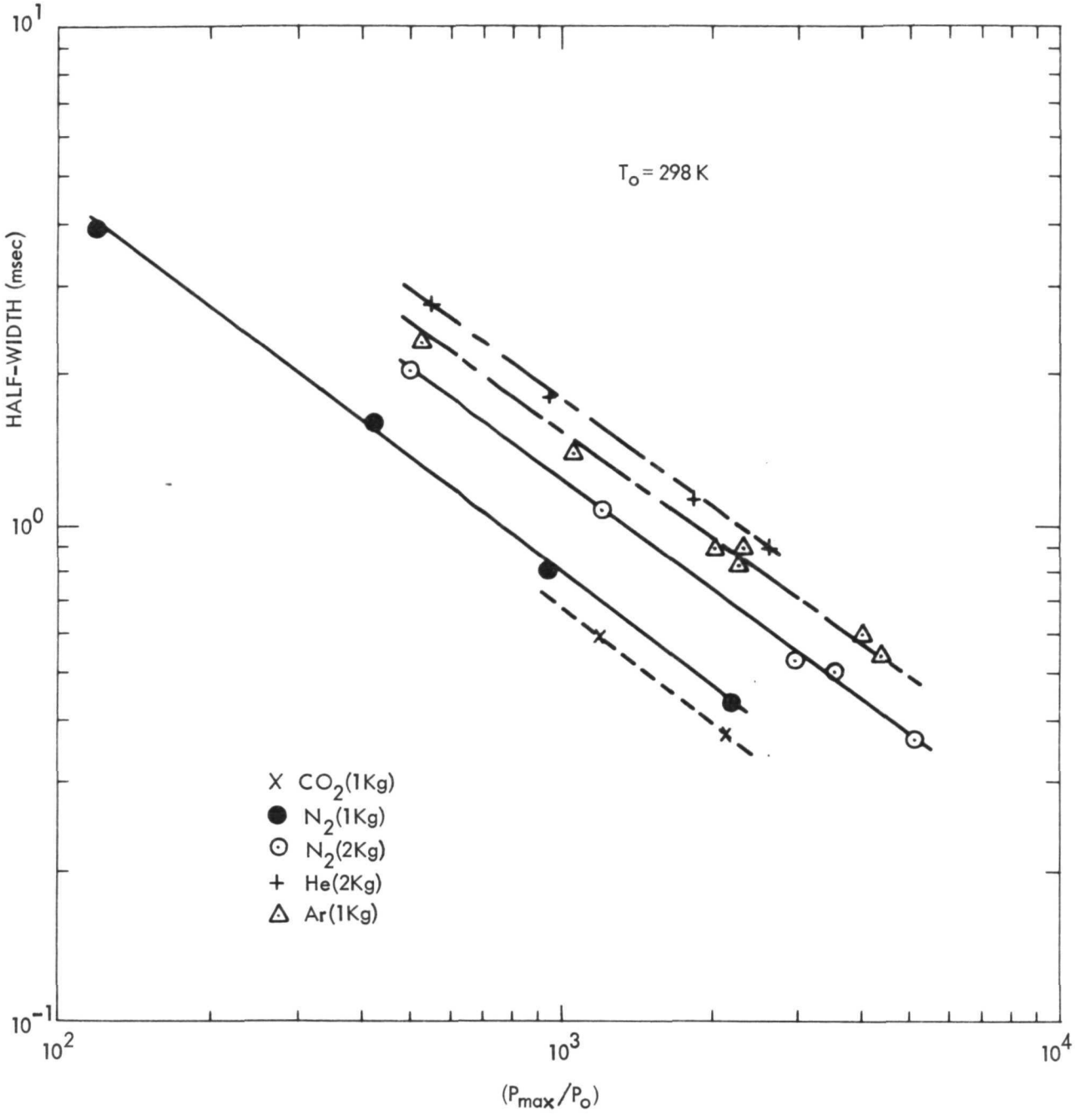

FIG. 8 PRESSURE PULSE WIDTH VS. COMPRESSION RATIO

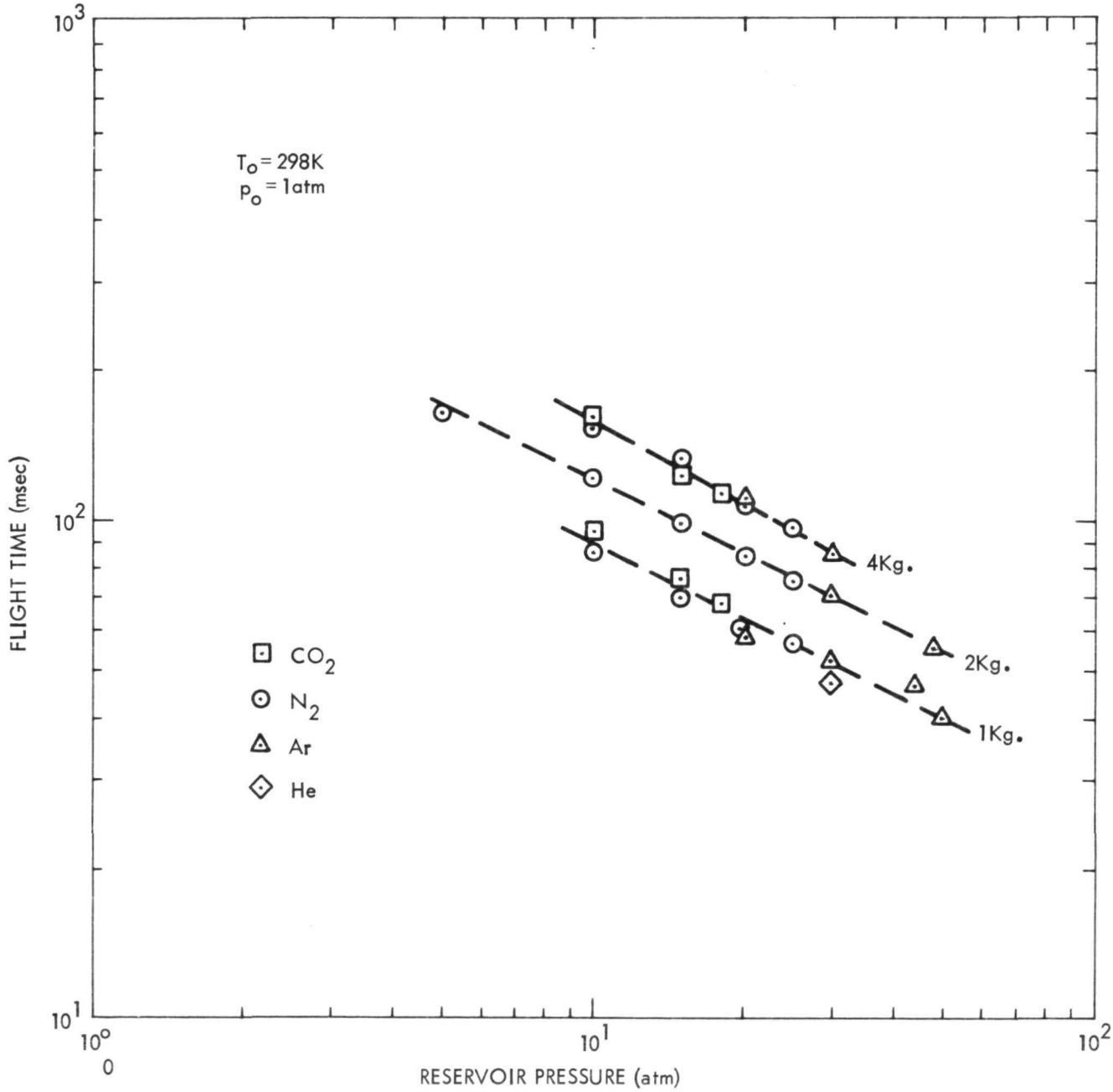

FIG. 9 PISTON FLIGHT TIME VS. RESERVOIR PRESSURE

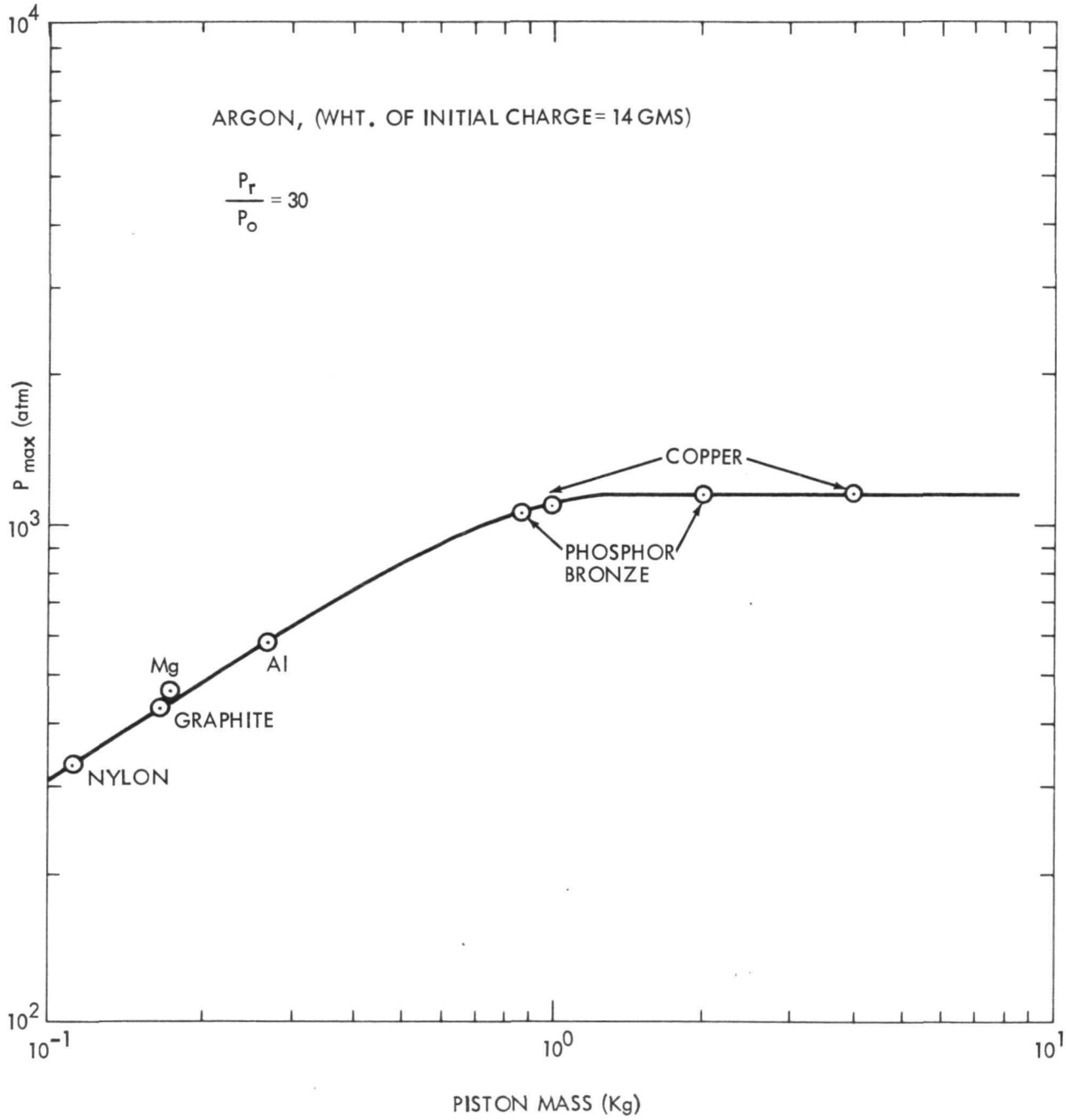

FIG. 10 MAXIMUM PRESSURE VS PISTON MASS

(a)

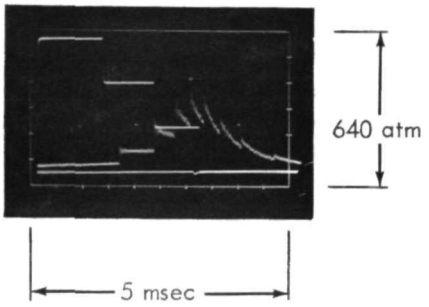

Mg PISTON, 0.173 Kg
$\frac{Presv}{Po}$ = 30, ARGON

(b)

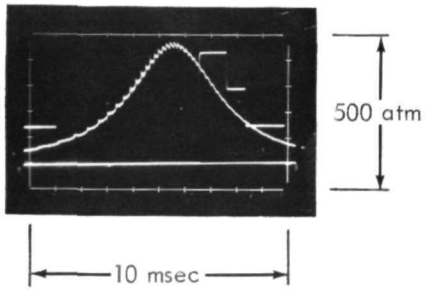

Cu PISTON, 4.0 Kg
$\frac{Presv}{Po}$ = 20, ARGON

(c)

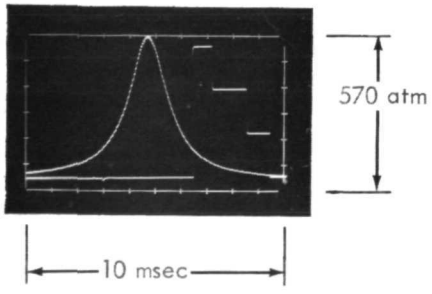

Cu PISTON, 1.0 Kg
$\frac{Presv}{Po}$ = 20, HELIUM

FIG. 11 PRESSURE-TIME RECORDS SHOWING SHOCK STRUCTURE

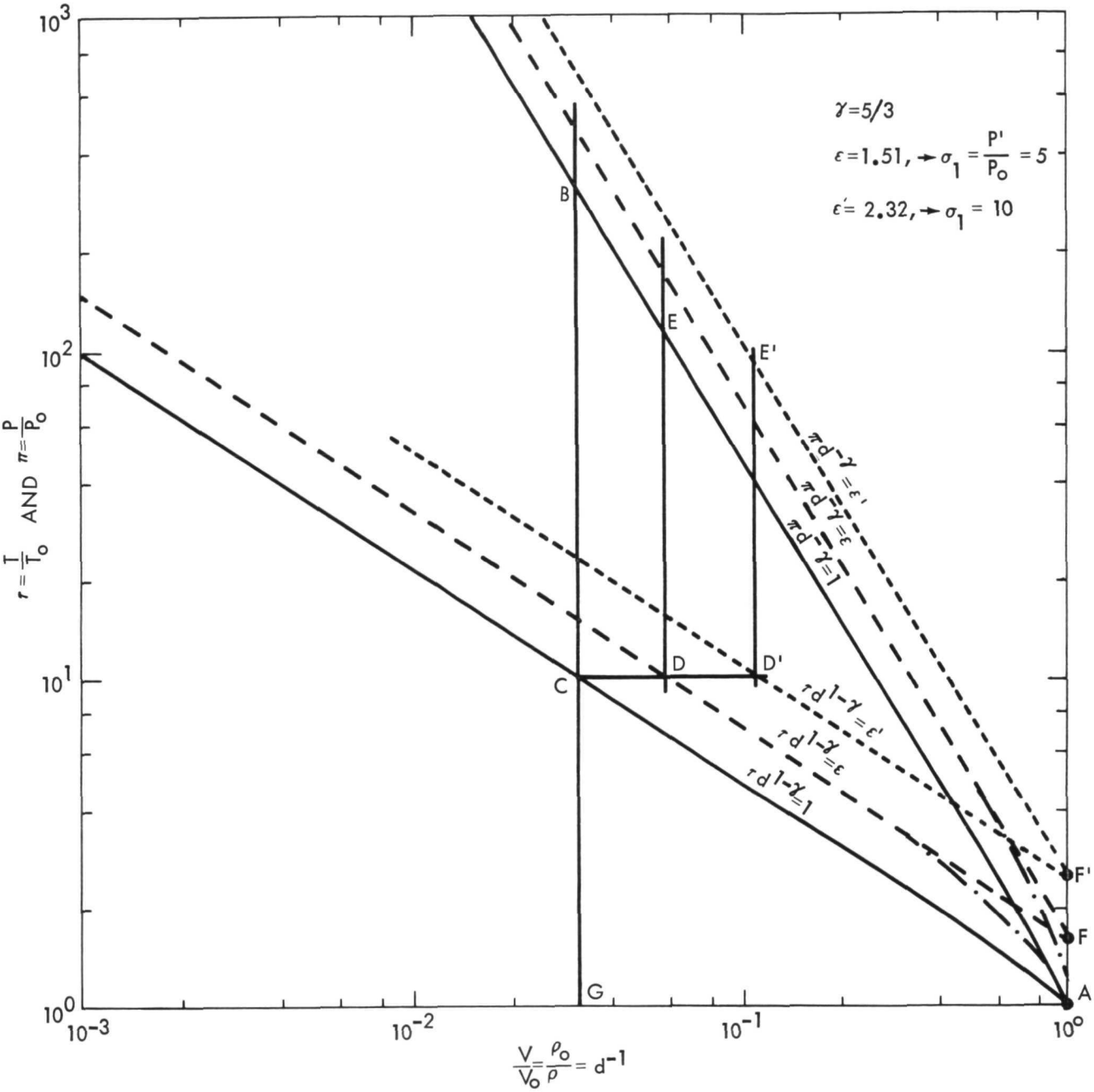

FIG. 12 PVT RELATIONS WITH AND WITHOUT SHOCK FORMATION

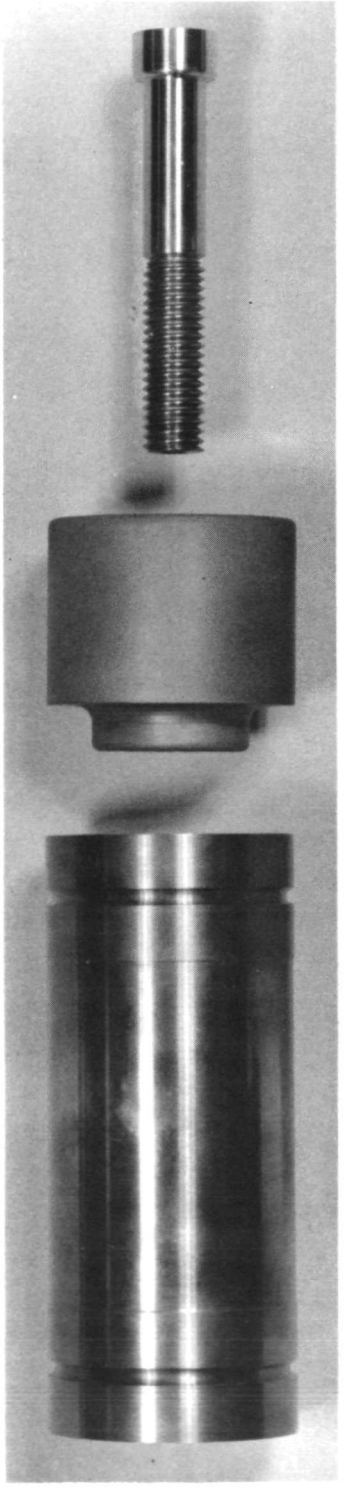

FIG. 13 DISASSEMBLED PISTON AND GRAPHITE HEAD

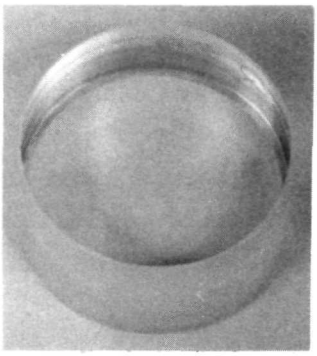

FUSED SILICA

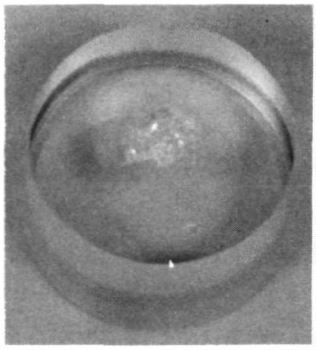

FUSED SILICA

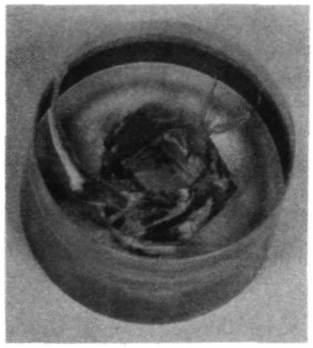

LUCITE

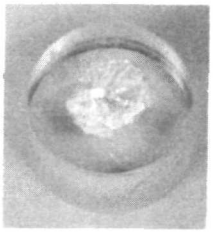

FUSED SILICA

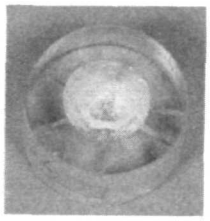

CORNING 70 70

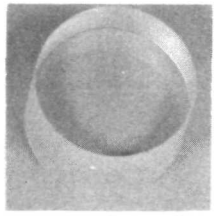

SYN. SAPPHIRE

FIG. 14 HIGH PRESSURE WINDOWS, AND SOME EXAMPLES OF FAILURE MODES

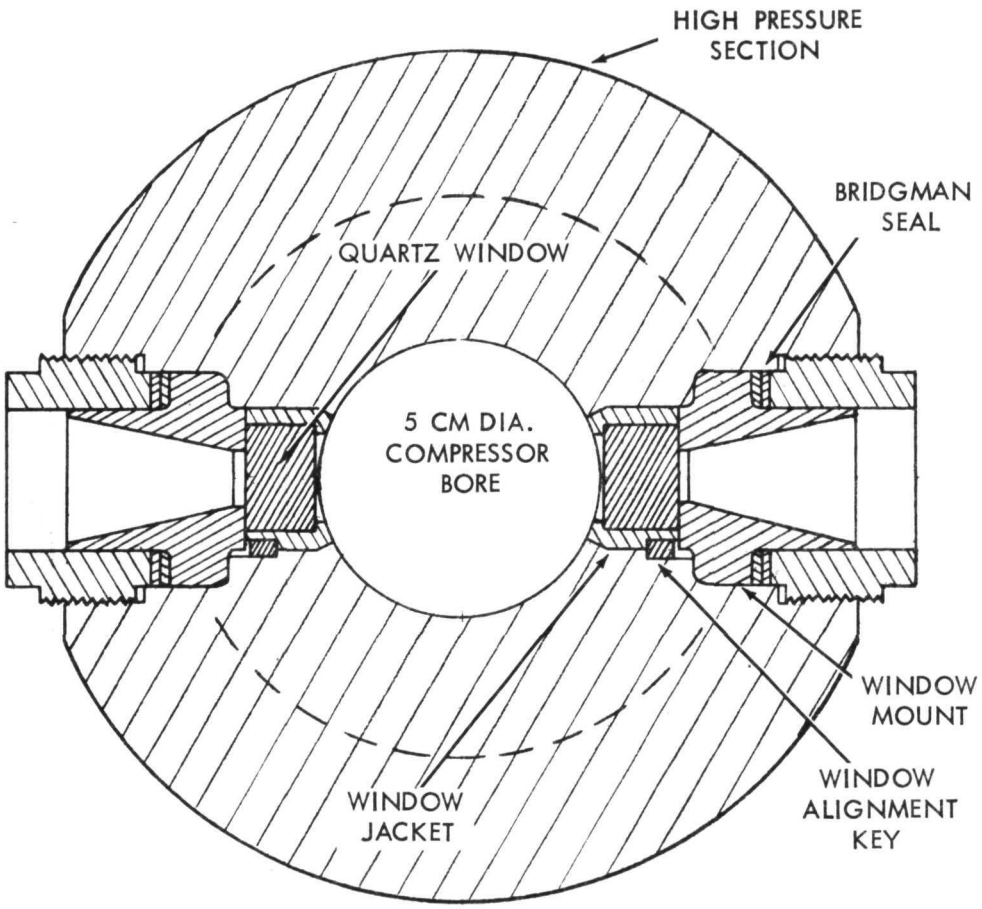

FIG. 15 DETAILS OF SIDE WINDOW TEST SECTION

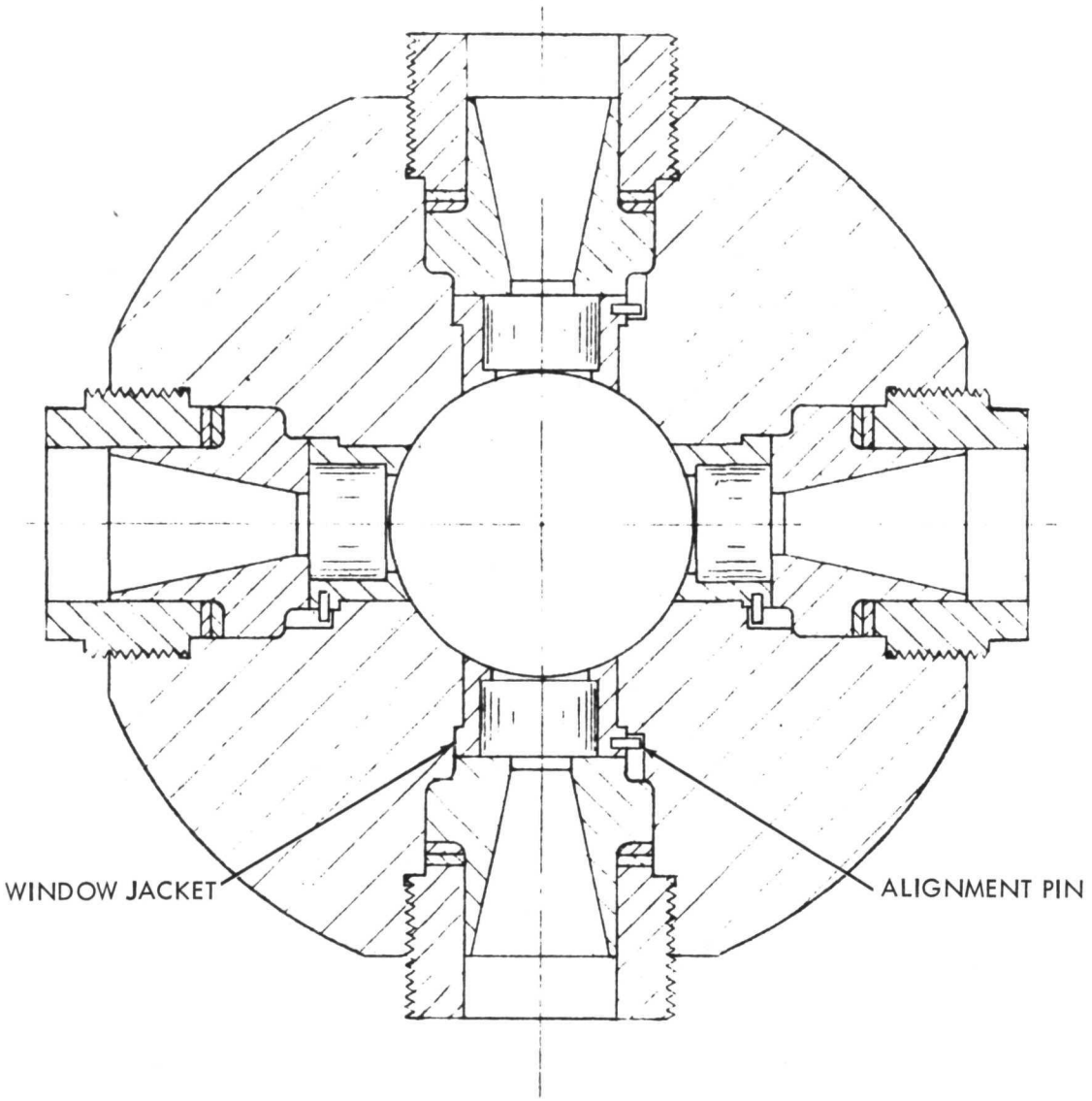

FIG. 16 4-PORT TEST SECTION DESIGN

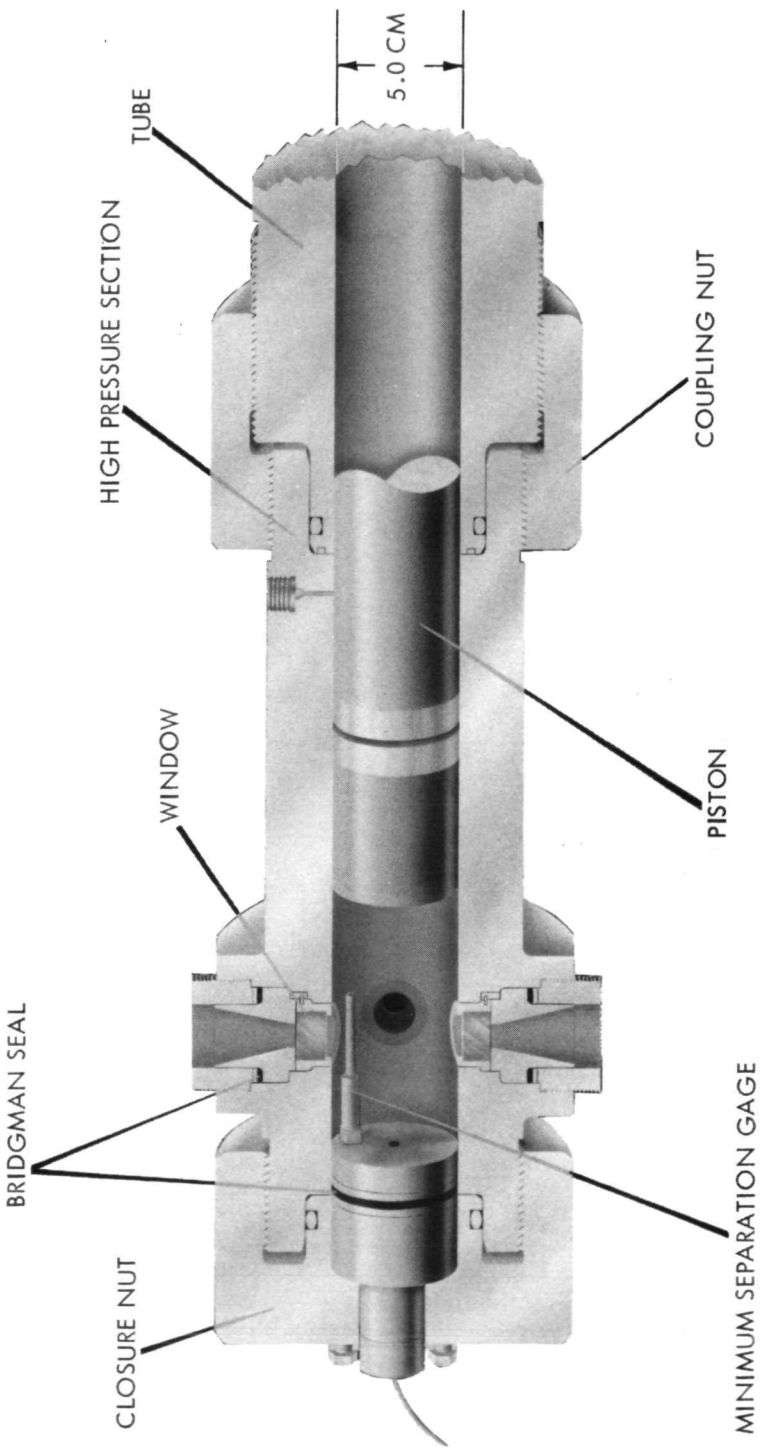

FIG. 17 4- PORT TEST SECTION ASSEMBLY WITH MINIMUM SEPARATION GAGE

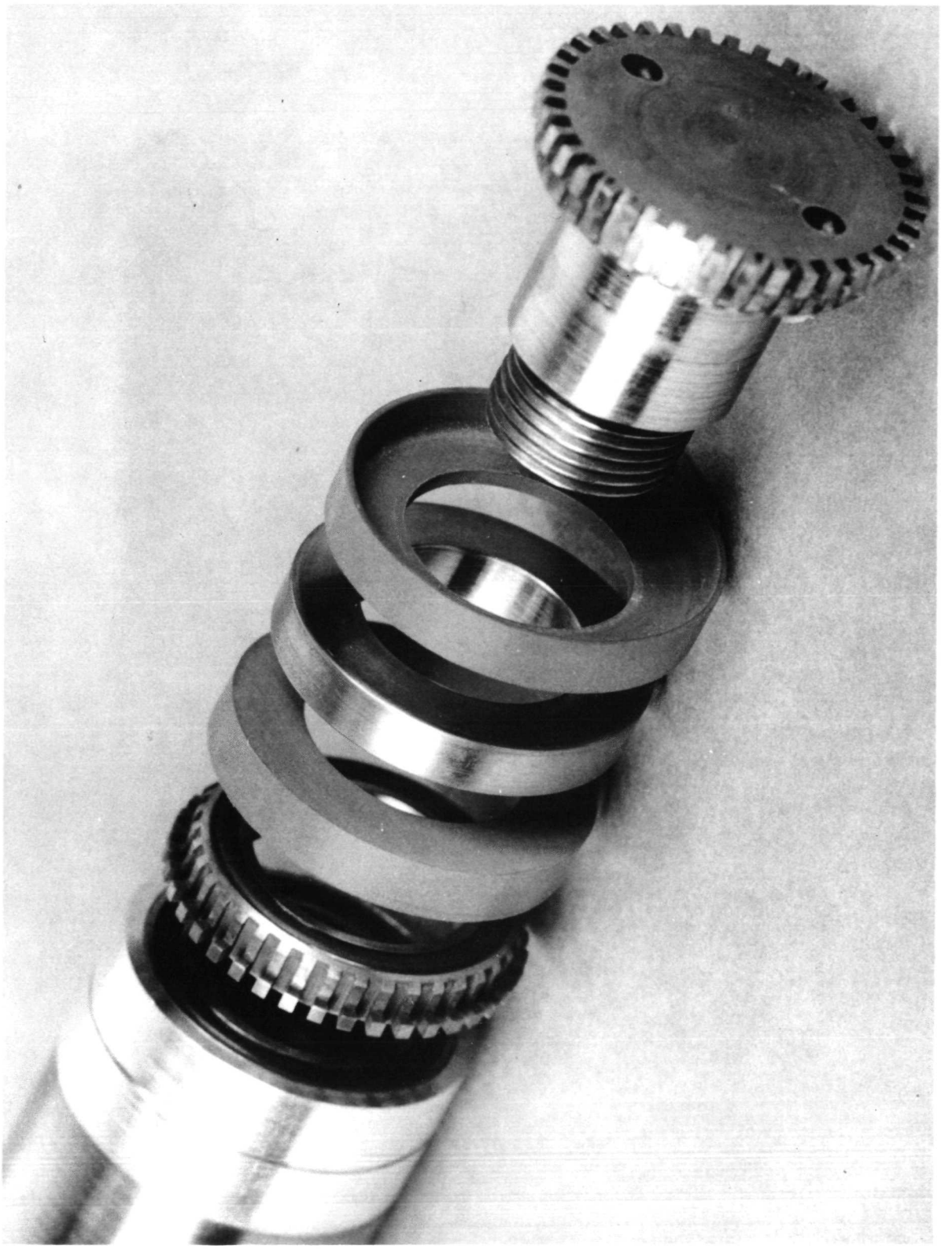

FIG. 18 PISTON SEAL ASSEMBLY

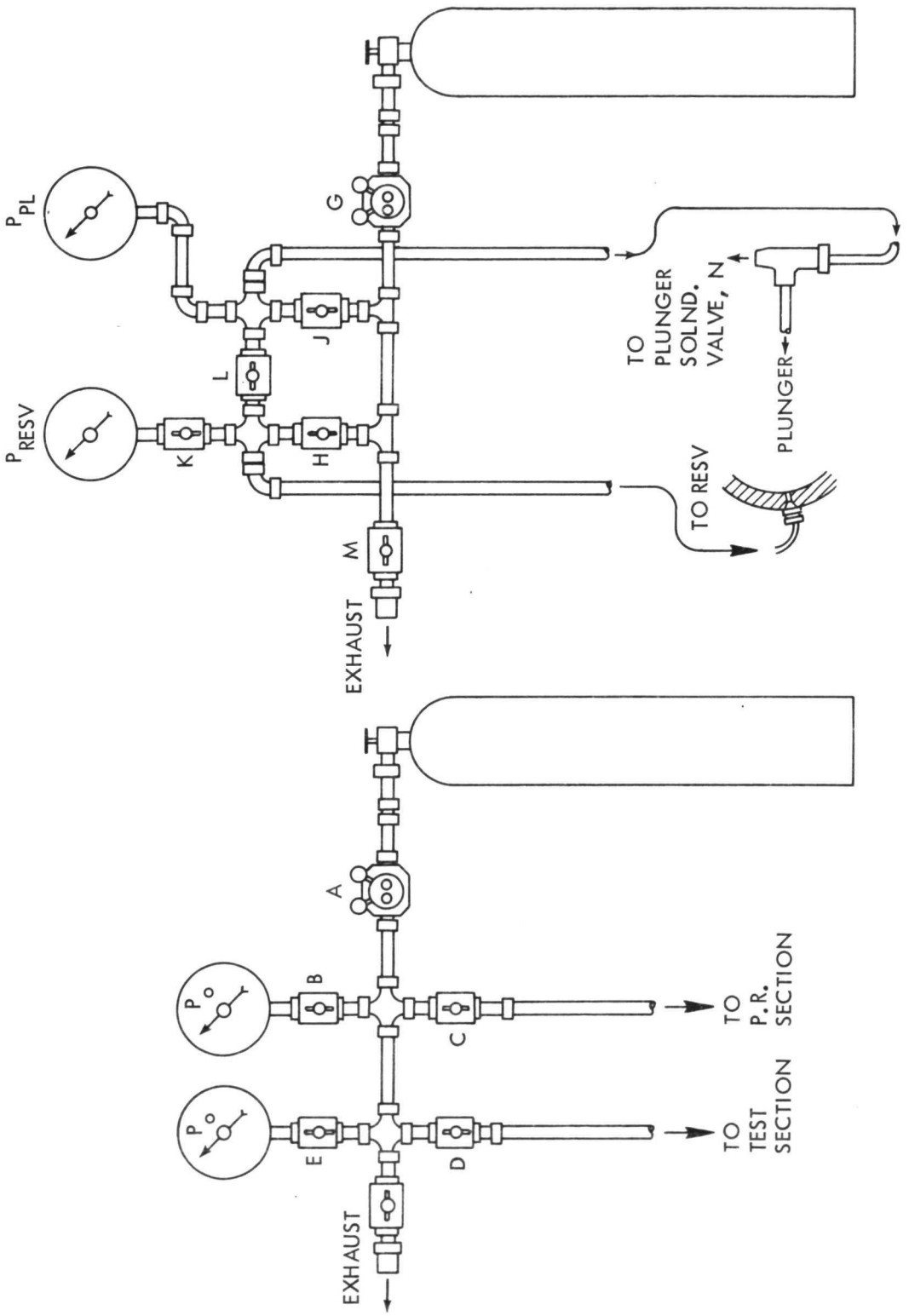

FIG. 19 REGULAR GAS-HANDLING SYSTEM

20

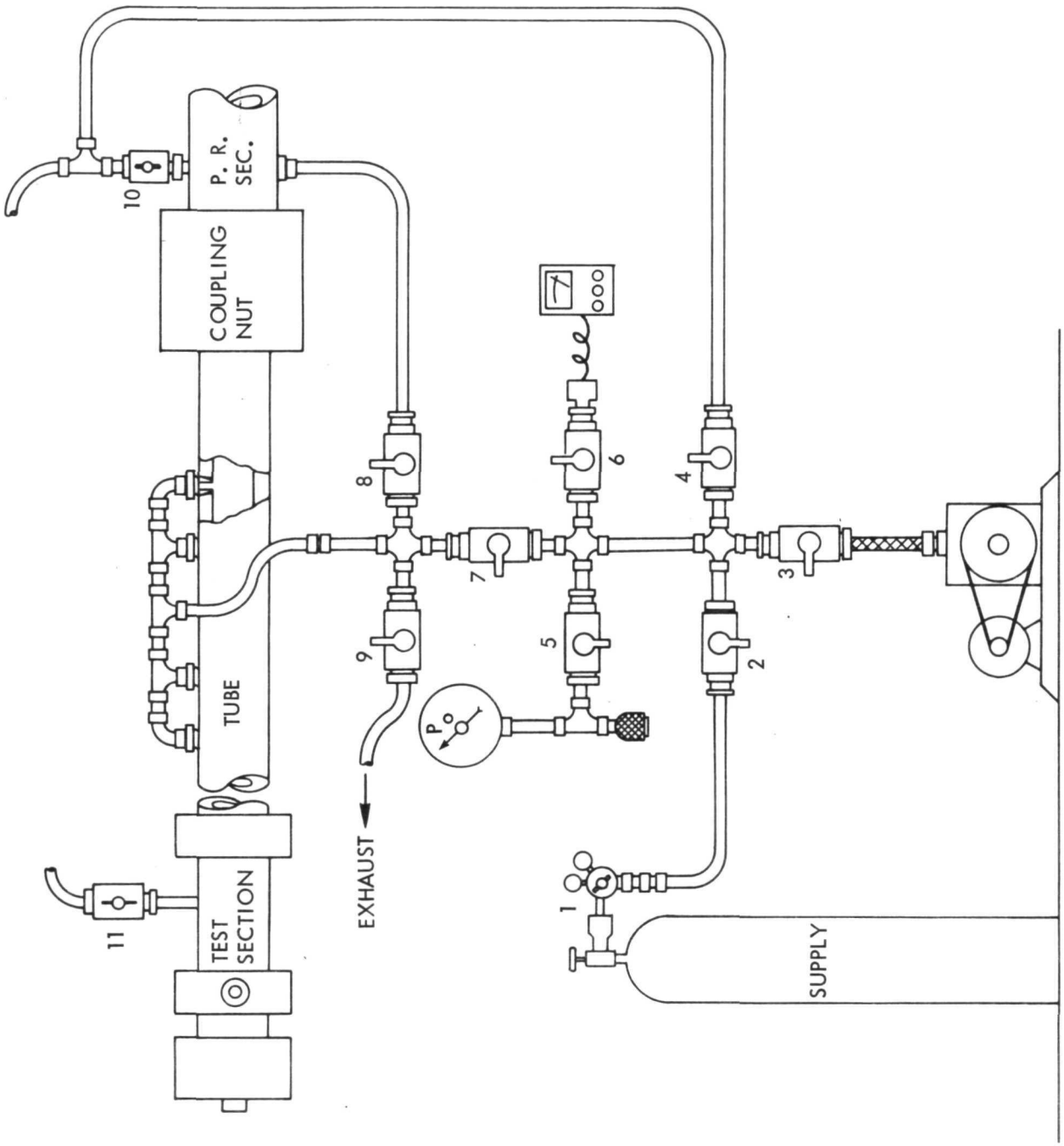

FIG. 20 HIGH PURITY GAS-HANDLING SYSTEM

DISTRIBUTION

	Copies
Office of Naval Research Washington, DC 20360 Code 421	2
Defense Documentation Center Cameron Station Alexandria, VA 22314	12
NASA-Lewis Research Center 21000 Brookpark Road Cleveland, OH 44135 Dr. R. W. Patch (106-1)	10
Naval Ordnance Systems Command Washington, DC 20360 ORD-03A	1
Dr. L. Merrill Asst. Director High Pressure Data Center P. O. Box 60, Univ. Station Provo, UT 84601	1
University of Maryland Department of Physics and Astronomy College Park, MD 20740 U. vanWijk Library	1
University of Oregon Physics Department Eugene, OR 97403 Prof. S. Y. Ch'en	1
Portland State College Physics Department Portland, OR 97207 Prof. M. Takeo	1
Harvard College Observatory 60 Garden Street Cambridge, MA 02138 Dr. D. D. Burgess	1
University of Florida Nuclear Engineering Department Gainsville, FL 32601 Dr. R. T. Schneider	1

DISTRIBUTION (Cont.)

	Copies
AEC-NASA Headquarters Code NS Washington, DC 20545 Dr. K. Thom	1
General Electric Company Research and Development Center Schenectady, NY 12305 Dr. Marshall Lapp	1

UNCLASSIFIED
Security Classification

DOCUMENT CONTROL DATA - R & D

Security classification of title, body of abstract and indexing annotation must be entered when the overall report is classified)

1. ORIGINATING ACTIVITY (Corporate author)	2a. REPORT SECURITY CLASSIFICATION
Naval Ordnance Laboratory White Oak, Silver Spring, Maryland 20910	UNCLASSIFIED
	2b. GROUP

3. REPORT TITLE

THE NOL BALLISTIC PISTON COMPRESSOR II.
OPERATION UP TO 5,000 ATM.

4. DESCRIPTIVE NOTES (Type of report and inclusive dates)

5. AUTHOR(S) (First name, middle initial, last name)

Gordon L. Hammond and George T. Lalos

6. REPORT DATE	7a. TOTAL NO. OF PAGES	7b. NO. OF REFS
16 December 1971	56	45

8a. CONTRACT OR GRANT NO. NASA	9a. ORIGINATOR'S REPORT NUMBER(S)
Interagency No. C-7757B	NOLTR 71-228
b. PROJECT NO. MAT-03L-00/ZR011-01-01	
c. Prob 167	9b. OTHER REPORT NO(S) (Any other numbers that may be assigned this report) NASA CR-120844
d.	

10. DISTRIBUTION STATEMENT

Approved for public release; distribution unlimited.

11. SUPPLEMENTARY NOTES	12. SPONSORING MILITARY ACTIVITY
	Chief of Naval Material Washington, D. C.

13. ABSTRACT

Experiments are described which demonstrated the feasibility of rapidly compressing inert gases in a ballistic piston compressor to simultaneously high temperatures and densities previously unobtainable in the laboratory. With argon, temperatures of the order of 6000°K and accompanying densities of the order of 100 Amagats have been obtained; and with nitrogen, temperatures and densities of 3000°K and 400 Amagats have been approached. Details of the design, assembly, instrumentation, and operating procedures are presented, and the results of mechanical and thermal performance tests up to 5000 atmospheres pressure are described. Emphasis is placed on experiments which demonstrated the usefulness of this apparatus for spectral line broadening studies.

DD FORM 1 NOV 65 1473 (PAGE 1)

S/N 0101-807-6801

UNCLASSIFIED
Security Classification

14 KEY WORDS	LINK A		LINK B		LINK C	
	ROLE	WT	ROLE	WT	ROLE	WT
Ballistic Piston Compressor Hot, Dense Gases Spectral Line Broadening						